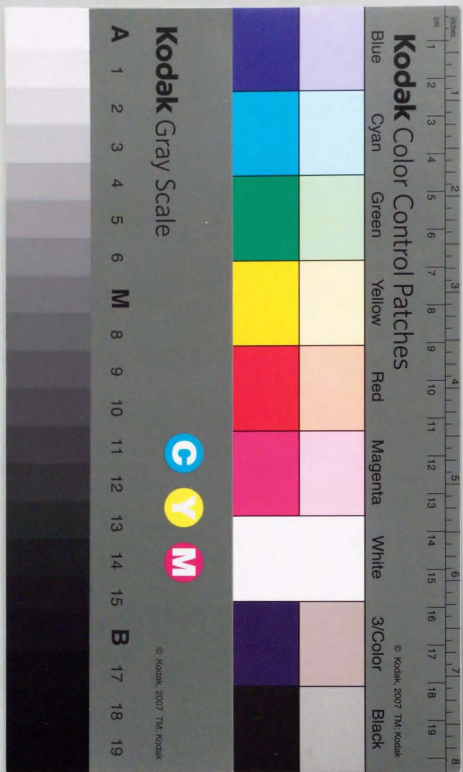Spin-Peierls Transition in CuGeO$_3$

（ CuGeO$_3$ のスピン・パイエルス転移 ）

長 谷 正 司

Doctor's Thesis

博士　論文

Spin-Peierls Transition in CuGeO$_3$

(CuGeO$_3$のスピン・パイエルス転移)

Masashi HASE

長谷　正司

Department of Applied Physics
The University of Tokyo

東京大学大学院工学系研究科
物理工学専攻

CONTENTS

[1] Introduction

Magnetic properties of low-dimensional systems of quantum spins with antiferromagnetic (AF) interactions have attracted much attention because of their various interesting phenomena, *e.g.*, the spin-Peierls (SP) transition in AF Heisenberg chains with 1/2 spins coupled to the three-dimensional (3D) phonon systems (Jacobs *et al.* 1976), the appearance of the Haldane gap in Heisenberg chains with integer spins (Haldane 1983a and 1983b, Renard *et al.* 1987, Katsumata *et al.* 1989 and Ajiro *et al.* 1989) and the high-temperature superconductivity occurring in layered cuprates including CuO_2 planes (Ginsberg 1992). In particular, AF oxides containing Cu^{2+} have been extensively studied (Cheong, Thompson and Fisk 1989) since the discovery of cuprate superconductors, because the two-dimensional (2D) CuO_2 planes are responsible for the high-temperature superconductivity. Our motivation to study the magnetic properties of $CuGeO_3$ including linear chains with Cu^{2+} is to compare one-dimensional (1D) Cu^{2+} based antiferromagnets with 2D cuprate superconductors. This compound is suitable for magnetic studies because only Cu^{2+} is magnetic ($S=1/2$).

In this Doctor's Thesis, I report the magnetic susceptibility of single-crystal $CuGeO_3$, which clearly exhibits the characteristic properties of the SP transition (Hase, Terasaki and Uchinokura 1993). As far as I know, the existence of this transition has been discovered for the first time in inorganic materials, while it has been observed so far in some organic compounds such as TTF-CuBDT (Bray *et al.* 1975) and MEM-$(TCNQ)_2$ (Huizinga *et al.* 1979).

In addition to this discovery, I have investigated magnetic properties of $CuGeO_3$ in high magnetic fields with using the magnetization measurements and compared the results with the data of organic SP materials and

1

theories (Hase *et al.* 1993a). In this study, I have succeeded in obtaining the magnetic phase diagram, which confirms the occurrence of the SP transition in this cuprate.

The effects of the impurity doping on the SP system have been also studied (Hase *et al.* 1993b). This study is the first report of the effects of impurities on the SP system. As is well known, the impurities doped in the AF quantum spin systems significantly affect its physical properties. For example, Cu doped in the Haldane material causes the $S = 1/2$ degrees of freedom at the edges (Hagiwara *et al.* 1990), while Zn doped in the high-T_c cuprate drastically suppresses its superconductivity (Maeda *et al.* 1990). On the contrary, the effect of impurities for the SP system has never been investigated. In organic SP materials, unpaired electrons on molecules such as TTF$^+$ or TCNQ$^-$ are responsible for localized spins ($S=1/2$). Thus the value of S on a part or all of these ions cannot be easily changed. On the other hand, I have succeeded in substitution of Zn^{2+} for Cu^{2+}. The magnetic susceptibilities of polycrystalline Cu$_{1-x}$Zn$_x$GeO$_3$ were measured. The SP transition temperature drastically reduces upon Zn doping and the SP transition was not observed around $x = 0.03$. The Zn-doping causes another phase transition in the samples with $0.02 \leq x \leq 0.08$, which proved to be spin-glass-like. Besides the magnetic susceptibility, I report the magnetic-field, temperature and x dependences of the magnetization of Cu$_{1-x}$Zn$_x$GeO$_3$ and the magnetic phase diagram (Hase *et al.* 1994).

I briefly summarize the SP transition. This transition may occur in a system with $S=1/2$ (or half-odd) Heisenberg-XY AF chains coupled to 3D phonons. In the SP system, both structural and magnetic properties change at T_{SP}. As is shown in Fig. 1-1, uniform Heisenberg AF linear chains undergo a transformation to dimerized AF linear chains. In the SP state, the value of the exchange interaction alternates according to the

dimerization of the lattice. In Fig. 1-2, I show magnetic-excitation spectra between the spin-singlet ground state and excited states in uniform and dimerized chains. The magnetic excitation is gapless at $k=0$ due to quantum fluctuations in uniform chains (des Cloizeaux and Pearson 1962, Johnson, Krinsky and McCoy 1973 and Bonner and Blöte 1982), while the ground state is spin-singlet (non-magnetic) and a finite energy gap opens in the excitation spectrum in dimerized chains. As for the spin system, the energy of the ground state of dimerized chains is lower than that of uniform chains. The SP transition occurs, if this energy gain of the spin system overcomes the increase of the energy of the lattice caused by the dimerization.
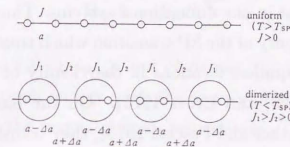

Fig. 1-1

Schematic pictures of uniform and dimerized chains, which include a position dependence of the exchange interaction J.
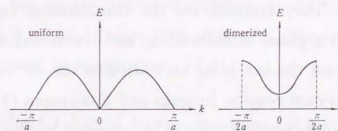

Fig. 1-2

Schematic magnetic-excitation-dispersion spectra for uniform and alternating Heisenberg antiferromagnetic chains.

In this section, I briefly summarize the theories related to the SP transition. In [2-1], the model Hamiltonian of the SP system is introduced (Pytte 1974), and the fundamental mechanism in the occurrence of the SP transition is explained with using the Jordan-Wigner transformation (Jordan and Wigner 1928) (the spinless-fermion representation) and a Hartree approximation for the spin system and a random phase approximation for the phonon system. However the Hartree approximation is inadequate to the treatment for the spin system, because quantum fluctuations are considered to be significant in one-dimensional systems. Thus Cross and Fisher have developed the theory of the SP transition which treats more accurately interactions between spinless fermions in the vicinity of the Fermi surface (Cross and Fisher 1979, and Cross 1979). On the basis of the Luther-Peschel treatment (Luther and Peschel 1975), they transformed the Hamiltonian represented by the spinless-fermion operators into that represented by density operators (boson operators), and obtained an exactly solvable model, which is equivalent to the Tomonaga-Luttinger model (Tomonaga 1950 and Luttinger 1963). Their theory is briefly described in [2-2]. In [2-3], I report the phase Hamiltonian developed by Nakano and Fukuyama (1980 and 1981). They transformed the Hamiltonian expressed by density operators into a phase Hamiltonian, and succeeded to treat properly the ground state and the low-lying excitation in the SP state. In addition to the above-mentioned results, Inagaki and Fukuyama (1983a, 1983b and 1984) obtained various phase diagrams represented by the parameters such as the spin-phonon coupling constant, interchain exchange interaction, the staggered field, the anisotropy of the exchange interaction and the magnetic field.

[2-1] Model Hamiltonian and Hartree approximation

The model Hamiltonian for the SP system is given as follows;

$$\mathbf{H} = \mathbf{H}_1 + \mathbf{H}_2 + \mathbf{H}_3, \qquad (2-1)$$

$$\mathbf{H}_1 = \sum_i J(i, i+1)\{\mathbf{S}_i \cdot \mathbf{S}_{i+1} - \frac{1}{4}\}, \qquad (2-2)$$

$$\mathbf{H}_2 = \hbar \sum_q \omega_q b_q^\dagger b_q, \qquad (2-3)$$

$$\mathbf{H}_3 = -g\mu_B H \sum_i S_i^z. \qquad (2-3)$$

The variables $J(i, i+1)$, ω_q, g and H denote the intrachain exchange interaction, the phonon energy with the wave-number q, the g-value of the isolated spin and the magnetic field, respectively. The constants $\hbar$ and μ_B denote the Planck constant and the Bohr magneton, respectively. The operators $\mathbf{S}_i$ and $b_q^\dagger(b_q)$ represent the spin operator at the i-th site and the phonon creation (annihilation) operator, respectively. The terms of $\mathbf{H}_1$, $\mathbf{H}_2$ and $\mathbf{H}_3$ mean the Hamiltonians for the spin system coupled to the phonon system, the phonon system and the Zeeman energy, respectively.

First of all, the spin system is considered. If the value of u_i (the shift of the i-th site) is much smaller than that of a (the lattice spacing), the term $\mathbf{H}_1$ is expanded as shown in eq. (2-4).

$$J(i, i+1) \sim J + (u_i - u_{i+1})\frac{\partial}{\partial u_i} J(i, i+1). \qquad (2-4)$$

Thus the Hamiltonian $\mathbf{H}_1$ is rewritten as follows;

$$\mathbf{H}_1 \sim \mathbf{H}_{11} + \mathbf{H}_{12}, \qquad (2-5)$$

$$\mathbf{H}_{11} = J \sum_i \{ \mathbf{S}_i \cdot \mathbf{S}_{i+1} - \frac{1}{4} \}, \qquad (2-6)$$

$$\mathbf{H}_{12} = \sum_i (u_i - u_{i+1}) \frac{\partial}{\partial u_i} J(i, i+1) \{ \mathbf{S}_i \cdot \mathbf{S}_{i+1} - \frac{1}{4} \}. \qquad (2-7)$$

The Hamiltonian expressed by the spinless-fermion operators is obtained by the Jordan-Wigner and Fourier transformations. Let us now consider the Heisenberg-XY Hamiltonian given in eq. (2-8).

$$\mathbf{H}'_{11} = J_\perp \sum_i (S_i^x S_{i+1}^x + S_i^y S_{i+1}^y) + J_z \sum_i S_i^z S_{i+1}^z. \qquad (2-8)$$

The operators $a_i^\dagger$ and a_i are defined in eqs. (2-9) and (2-10).

$$S_i^+ = (S_i^-)^\dagger = \exp\{ -i\pi \sum_j^{i-1} a_j^\dagger a_j \} a_i^\dagger \qquad (2-9)$$

$$S_i^z = a_i^\dagger a_i - \frac{1}{2} \qquad (2-10)$$

Since the spin operators have the commutation relation $[S^k, S^l] = i\epsilon_{klm} S^m$, the following anticommutation relations are derived.

$$\{ a_i^\dagger, a_{i'} \} = \delta_{ii'} \qquad (2-11)$$

$$\{ a_i^\dagger, a_{i'}^\dagger \} = \{ a_i, a_{i'} \} = 0 \qquad (2-12)$$

With using eqs. (2-9) and (2-10), and the Fourier transformation

$$a_j^\dagger = N^{-\frac{1}{2}} \sum_k \exp(-ikja) a_k^\dagger, \qquad (2-13)$$

the following Hamiltonian is obtained,

$$\mathbf{H}'_{11} = \sum_k \epsilon_k a_k^\dagger a_k + N^{-1} \sum_{kk'q} v_q a_{k+q}^\dagger a_{k'-q}^\dagger a_{k'} a_k, \qquad (2-14)$$

6

where

$$\epsilon_k = J_\perp \{ \cos(ka) - 1 \},$$

$$v_q = J_z \cos(qa). \qquad (2-15)$$

The first and second terms of r.h.s. of $\mathbf{H}'_{11}$ denote the kinetic energy of the spinless fermions and the interaction energies between the spinless fermions. Since the magnetization is 0, i.e., $N^{-1} \sum_i < S_i^z >= 0$ in the absence of H, the following relation is obtained.

$$N^{-1} \sum_k < a_k^\dagger a_k >= N^{-1} \sum_i < a_i^\dagger a_i >= \frac{1}{2}. \qquad (2-16)$$

The eq. (2-16) means that the band of the spinless fermions is half-filled.

In order to obtain a solvable model, a Hartree Approximation is used. Assuming eq. (2-17) and using self-consistently solvable eqs. (2-18) $\sim$ (2-20), the Hamiltonian (2-21) is obtained (now $J_\perp = J_z = J$).

$$< a_k^\dagger a_{k'} >= n_k \delta_{kk'}, \qquad (2-17)$$

$$n_k = \{ \exp(\beta E_k) + 1 \}^{-1}, \qquad (2-18)$$

$$E_k = pJ \cos(ka), \qquad (2-19)$$

$$p = 1 - \frac{2}{N} \sum_k n_k \cos(ka), \qquad (2-20)$$

$$\mathbf{H}_{11} \to \sum_k E_k a_k^\dagger a_k. \qquad (2-21)$$

With using (2-22) and the Jordan-Wigner transformation, the Hamiltonian $\mathbf{H}_{12}$ is changed as follows;

$$u_j = (MN)^{-\frac{1}{2}} \sum_q \exp(iqja)(b_q + b_{-q}^\dagger), \qquad (2-22)$$

7

$$\mathbf{H}_{12} \to \sum_{kq} g(k,q)(b_q + b_{-q}^\dagger)a_k^\dagger a_{k-q}, \qquad (2-23)$$

where $g(k,q)$ denotes the spin-lattice-coupling strength;

$$g(k,q) = 2ig(q)p\sin(ka) \qquad (2-24)$$

$$g(q) = (MN)^{-\frac{1}{2}}\frac{\partial}{\partial u_i}J(i,i+1) \qquad (2-25)$$

As a result, the Hamiltonian for the SP system is given as follows;

$$\mathbf{H} = \sum_k (E_k - g\mu_B H)a_k^\dagger a_k + \frac{1}{2}Ng\mu_B H + \sum_{kq} g(k,q)(b_q + b_{-q}^\dagger)a_k^\dagger a_{k-q}$$

$$+ \hbar\sum_q \omega_q b_q^\dagger b_q. \qquad (2-26)$$

This Hamiltonian is equivalent to that of the Peierls system.

The phonon energy changes due to the spin-lattice coupling. The transformed phonon energy is obtained on the basis of a random phase approximation.

$$\Omega_q^2 = \omega_q^2 + \Pi(q,\Omega_q), \qquad (2-27)$$

$$\Pi(q,\Omega_q) = \sum_k |g(k,q)|^2 \frac{n_k - n_{k-q}}{\Omega_q - E_{k-q} + E_k}. \qquad (2-28)$$

$\Pi(q,\Omega_q)$ is the polarizability due to the spin-lattice coupling. Considering the nesting condition, a phase transition characterized by $\Omega_{2k_F} = 0$ occurs, and this transition is the SP transition. In Fig. 2-1, dispersion curves of the spinless fermions above and below the SP transition temperature (T_{SP}) are shown. Below T_{SP}, an energy gap opens at the Fermi surface. From eqs. (2-27) and (2-28), the value of T_{SP} is determined as follows;

$$T_{SP} = J\exp(-\lambda^{-1}), \qquad (2-29)$$

$$\lambda = \frac{|g(2k_F)|^2}{J\omega_{2k_F}^2}. \qquad (2-30)$$
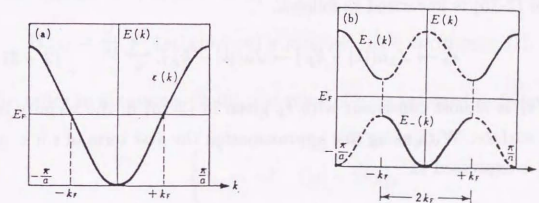
8

Fig. 2-1

The dispersion relations of the spinless fermions. (a) $T > T_{SP}$ and (b) $T < T_{SP}$.

9

As is above-mentioned, the spin fluctuations cannot be properly treated in the calculation with the Hartree approximation. Therefore some problems occur owing to this approximation. For example, the formula of T_{SP} is considered to be invalid. In 1979, Cross and Fisher have developed a new theory. In this section, their theories are briefly summarized.

At low temperatures, the properties of the fermion system such as the behavior of the response function are considered to be mainly determined by low-energy excitations near the Fermi surface. In their theory, the term ϵ_k given in (2-15) is linearized as follows.

$$\epsilon_k \to J_\perp a(|k| - k_F) \to Ja(|k| - k_F). \qquad (2-31)$$

This new ϵ_k is almost consistent with ϵ_k given in (2-15) in the vicinity of the Fermi surface. With using this approximation the first term of r.h.s. of eq. (2-14) is expressed as

$$\mathbf{H}_0 \equiv \sum_k \epsilon_k a_k^\dagger a_k = Ja \sum_k k(a_{1k}^\dagger a_{1k} - a_{2k}^\dagger a_{2k}). \qquad (2-32)$$

The fermions with wave-vector $k \sim k_F$ and $k \sim -k_F$ are indicated as 1 and 2, respectively. Let us now identify $\mathbf{H}'_0$ which obeys the same commutation relation as $\mathbf{H}_0$.

$$\mathbf{H}'_0 = Ja \frac{2\pi}{L} \sum_{q<0} \{\rho_1(q)\rho_1(-q) + \rho_2(-q)\rho_2(q)\}. \qquad (2-33)$$

The operators $\rho_i(q)$ denote the density operators,

$$\rho_1(q) = \sum_{k>0} a_{1k+q}^\dagger a_{1k}, \qquad (2-34)$$

$$\rho_1(-q) = \sum_{k>0} a_{1k}^\dagger a_{1k+q}, \qquad (2-35)$$

$$\rho_2(q) = \sum_{k<-q} a_{2k+q}^\dagger a_{2k}, \qquad (2-36)$$

$$\rho_2(-q) = \sum_{k<-q} a_{2k}^\dagger a_{2k+q}. \qquad (2-37)$$

These density operators satisfy the following commutation relations,

$$[\rho_1(-q), \rho_1(q')] = [\rho_2(q'), \rho_2(-q)] = \frac{qL}{2\pi}\delta_{q,q'}, \qquad (2-38)$$

$$[\rho_1(q), \rho_2(q')] = 0. \qquad (2-39)$$

The second term of r.h.s. of eq. (2-14) is transformed in the same manner.

$$\mathbf{H}'_{int} = \frac{J}{N} \sum_q \{\rho_1(q)\rho_1(-q) + \rho_2(q)\rho_2(-q) + 4\rho_1(q)\rho_2(-q)\}. \qquad (2-40)$$

In order to obtain eq. (2-40), the value of v_q is assumed as follows;

$$\begin{cases} v_q = J & (|q| \sim 0 \ or \ 4k_F), \\ v_q = -J & (|q| \sim 2k_F), \\ v_q = 0 & (\text{otherwise}). \end{cases} \qquad (2-41)$$

Although the detailed calculations are omitted, the polarizability at $q \to 2k_F$ and $\Omega_{2k_F} \to 0$ is given in eq. (2-42).

$$\Pi(2k_F, 0) = -1.04|g(2k_F)|^2 T^{-1}. \qquad (2-42)$$

Thus T_{SP} is obtained as shown in eq. (2-43).

$$T_{SP} = 0.8J\lambda', \qquad (2-43)$$

where

$$\lambda' = \frac{4|g(2k_F)|^2}{\pi\omega_{2k_F}^2}. \qquad (2-44)$$

[2-3] Phase Hamiltonian

In the following paragraphs, I briefly introduce the phase Hamiltonian method which has been developed by Nakano, Inagaki and Fukuyama, and summarize their results.

Nakano and Fukuyama (1980 and 1981) have obtained the Hamiltonian expressed in terms of the following phase variables.

$$\begin{cases} \theta(x) = \theta_+(x), \\ p(x) = -\dfrac{1}{4\pi}\nabla\theta_-(x), \end{cases} \tag{2-45}$$

$$\theta_\pm(x) = i\sum_{q\neq 0}[\rho_1(q) \pm \rho_2(q)]\frac{2\pi}{Lq}\exp(-\frac{\alpha_c}{2}|q| - iqx). \tag{2-46}$$

These operators satisfy the following commutation relations,

$$[\theta(x), p(x')] = i\delta(x - x'). \tag{2-47}$$

The Hamiltonian is transformed as follows;

$$\mathbf{H} = \sum_i J(i, i+1)\mathbf{S}_i \cdot \mathbf{S}_{i+1} + \frac{K}{2}\sum_i (u_i - u_{i+1})^2$$

$$\Downarrow$$

$$\mathbf{H} = \int dx\left[A\{\nabla\theta(x)\}^2 + Cp^2(x) - B\sin\{\theta(x)\} - D\cos\{2\theta(x)\} + \frac{2K}{a}u^2\right], \tag{2-48}$$

where

$$A = \frac{Ja}{8}, \tag{2-49}$$

$$B = \frac{J\lambda u}{a^2}, \tag{2-50}$$

$$C = \frac{\pi^2 Ja}{2}, \tag{2-51}$$

$$D = \frac{\pi^2 J}{8a}, \tag{2-52}$$

The spin operator $S^z(x)$ is represented by phase variables as follows.

$$S^z(x) = \frac{1}{a}\cos\{\frac{\pi}{a}x + \theta(x)\} + \frac{1}{2\pi}\nabla\theta(x). \tag{2-53}$$

If $\theta(x) = 0$, $S^z(x = la) = (1/a) \times (-1)^l$. Therefore the state that $\theta(x) = 0$ indicates the Néel state. On the other hand, if $\theta(x) = \pi/2$, $S^z(x = la) = 0$. Thus the state that $\theta(x) = \pi/2$ corresponds to the spin-singlet state. Assuming that there exists a lattice distortion, this state represents the SP state. The characteristic advantage of the phase Hamiltonian is that various states such as the SP, Néel and incommensurate states can be treated in the same manner.

Although I omit the detailed analyses, the various phase diagrams obtained by the phase Hamiltonian are shown in Figs. 2-2 $\sim$ 2-4.

(1) the spin-lattice coupling *versus* the Ising anisotropy ($\lambda\sqrt{\frac{J}{Ka^2}}$ *vs.* $\epsilon = \frac{J_z}{J} - 1$) (Fig. 2-2) (Inagaki and Fukuyama 1983a)

As the Ising anisotropy increases, the Néel state appears. However the SP state is stable in a wide region of parameters in this figure.

(2) the spin-lattice coupling *versus* the interchain exchange interaction ($\eta = \frac{J\lambda^2}{4\pi^2 Ka^2}$ *vs.* $j' = \frac{z|J'|}{\pi^2 J}$) (Fig. 2-3) (Inagaki and Fukuyama 1983b).

As the interchain exchange interaction increases, the Néel state appears. This result indicates that the SP state becomes unstable for the interchain exchange interaction.

(3) the magnetic field *versus* the interchain exchange interaction (h/η *vs.* j'/η) (Fig. 2-4) (Inagaki and Fukuyama 1984)

This figure clearly shows that the magnetic discommensurate (MD) state appears above a high field. In addition to this, it should be noted

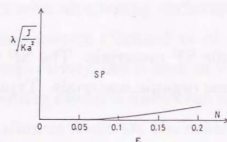that the field representing the phase boundary between the SP and MD phases reduces with increasing j'.

Fig. 3. Schematic diagram of stable states; SP: the spin-Peierls state, N: the Néel state. $\varepsilon = J_z/J - 1$.
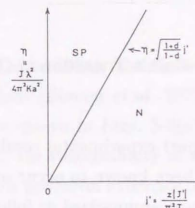

Fig. 1. Phase diagram of stable states in the case of the interchain exchange interaction in SCHA; SP: the spin-Peierls state, N: the Néel state. The ordinate η is the dimensionless spin-lattice coupling, eq. (3.21), and the abscissa j' the dimensionless interchain exchange interaction, eq. (3.19).

Fig. 2-2

The phase diagram obtained in the theory of the phase Hamiltonian. The spin-lattice coupling *versus* the Ising anisotropy (Inagaki and Fukuyama 1983a).

Fig. 2-3

The phase diagram obtained in the theory of the phase Hamiltonian. The spin-lattice coupling *versus* the interchain exchanbge interaction (Inagaki and Fukuyama 1983b).
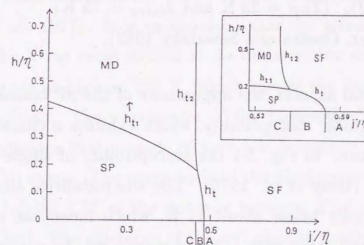

Fig. 3. Phase diagram of stable states in the presence of the magnetic field. The ordinate h/η denotes the magnetic field vs spin-lattice coupling, and the abscissa j'/η the interchain interaction vs spin-lattice coupling. Here we take $d = 0.5$.

Fig. 2-4

The phase diagram obtained in the theory of the phase Hamiltonian. The magnetic field *versus* the interchain exchange interaction (Inagaki and Fukuyama 1984).

[3] Spin-Peierls Transition in Organic Compounds

I report experimental results of organic SP materials. The SP transition has been known to occur so far in some organic materials. Typical SP systems are summarized as follows.

TTF-CuBDT ($T_{SP} = 11$ K and $J_{intra} = 77$ K)
(Bray $et\ al.$ 1975).
TTF-AuBDT ($T_{SP} = 2.0$ K and $J_{intra} = 68$ K)
(Jacobs $et\ al.$ 1976).
TTF-CuBDSe ($T_{SP} = 6$ K and $J_{intra} = 88$ K)
(Interrante $et\ al.$ 1979).
MEM-(TCNQ)$_2$ ($T_{SP} = 18$ K and $J_{intra} = 106$ K)
(Huizinga $et\ al.$ 1979).
DEM-(TCNQ)$_2$ ($T_{SP} = 23$ K and $J_{intra} = 75$ K)
(Schwerdtfeger, Oostra and Sawatzky 1982).

In experimental aspects, the appearance of the SP transition was confirmed in the magnetic susceptibility, which exhibits a characteristic temperature dependence. In Fig. 3-1 the susceptibility of single-crystal TTF-CuBDT is shown (Bray $et\ al.$ 1975). The suscptibilities along two directions decrease rapidly below about 11 K, which means an existence of a nonmagnetic ground state with a finite energy gap in a magnetic excitation spectrum. The data is isotropic in the whole measured temperature. It should be noted that the susceptibility above T_{SP} quantitatively agrees with the theoretical curve calculated by Bonner and Fisher (1964), which strongly indicates a 1D magnetic system. The susceptibility of the SP material is compared with those of other systems. The susceptibilities of the

1D-AF Heisenberg model (Bonner and Fisher 1964), the Heisenberg AF chains with alternating exchange interactions (Bonner $et\ al.$ 1979) and the Haldane system (Renard $et\ al.$ 1987) are shown in Figs. 3-2(a), (b) and (c), respectively. As is seen in Fig. 3-2 (a), the susceptibility of the 1D-AF Heisenberg model is finite even at 0 K, which means an existence of a gapless excitation at $k=0$. On the other hand, the susceptibilities of the latter two systems drop drastically to small valus at low temperatures, which is the common characteristic of the system having a nonmagnetic ground state with a finite energy gap in the magnetic excitation spectrum.

A lattice dimerization below T_{SP} was observed in organic SP compounds (TTF-CuBDT: Moncton $et\ al.$ 1977 and Kasper and Moncton 1979; MEM-(TCNQ)$_2$: van Bodegom, Larson and Mook 1981). Figure 3-3 shows the X-ray diffraction pattern of TTF-CuBDT (Moncton $et\ al.$ 1977). New Bragg peaks appear below T_{SP} and the temperature-dependent intensity of the new peak is accurately fitted by the BCS gap function (Fig. 3-4; Moncton $et\ al.$ 1977). It is emphasized that the strong diffuse scattering dominates the X-ray cross section at the dimerization superlattice positions for temperature as high as 225 K, which means the fluctuations preceding the SP transition. The persistence of the pronounced peak to high temperatures indicates that a mode of very low frequency (soft phonon mode; $\hbar\omega_0 \sim 1$ meV) exists. The magnitude of the displacement was estimated to be 0.072 Å (about 1 % of the distance between TTF molecules along the chain direction). The existence of the soft phonon mode in MEM-(TCNQ)$_2$ was also observed by far infrared spectroscopy (Tanaka, Satoh and Nagasaka 1990).

Among many experimental and theoretical works of the SP system, an investigation of this system in magnetic fields (H) is one of the most stimulative studies, because the organic SP materials exhibit characteristic

properties in H below $T_{SP}(0)$ (T_{SP} without H) (Bray *et al.* 1979, Bloch *et al.* 1980 and 1981, Northby *et al.* 1982a and 1982b, Hijmans, Brom and de Jongh 1985, de Jongh *et al.* 1986 and Bonner *et al.* 1987). In the absence of H, the wave vector of a lattice distortion (q) is π/a (a is a lattice spacing in a chain), which causes the lattice dimerization. In the SP system, as temperature (T) is lowered, a phase with uniform chains (U phase) are transformed into a phase with dimerized or alternating chains (D phase) at the transition temperature in a weak H. When the magnetic field is applied to the SP system, the value of q sticks at π/a in low magnetic fields on account of umklapp effects. However, another magnetic phase (M phase) appears above a critical field (H_c) and is considered to be an incommensurate phase. In Fig. 3-5, the H dependence of the magnetization of TTF-AuBDT is shown (Northby *et al.* 1982a). Below $T_{SP}(0)$, a rapid change of the magnetization was observed, which indicates a phase transition between the D and other phases. The M phase is different from the U phase, because the phase transition between the M and U phases was found in the T dependence of the differential susceptibility (Fig. 3-6; Northby *et al.* 1982a) and the specific heat (Fig. 3-7; Bonner *et al.* 1987) measured in various fields. As for the M phase, Hijmans, Brom and de Jongh (1985) have asserted that their results of NMR experiments can be explained in terms of a soliton-lattice model (Fig. 3-8).

It was claimed that typical organic SP materials show a universal behavior for the magnetic phase diagrams represented in terms of reduced variables $T/T_{SP}(0)$ and $H/T_{SP}(0)$ (Fig. 3-9; Northby *et al.* 1982a). The experimentally obtained phase boundaries between U and the other phases are of second order, and are consistent with the theoretical result of Cross (1979). On the other hand, the transition between D and M phases (DM transition) is of first order in a low-temperature region $[T/T_{SP}(0) \leq 0.5 \sim 0.7]$.
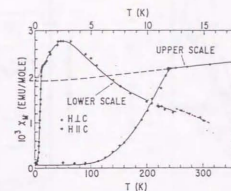

FIG. 2. Magnetic susceptibility of TTFCuS$_4$C$_4$(CF$_3$)$_4$ along two directions. Solid lines are calculated from a spin-Peierls theory, which contains AF chains with uniform exchange above 12 K and temperature-dependent alternating exchange below.

Fig. 3-1

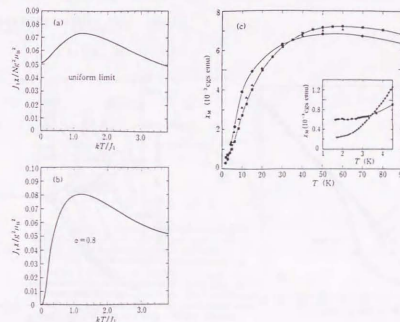The magnetic susceptibility of single-crystal TTF-CuBDT (Bray *et al.* 1975).

Fig. 3-2

(a) magnetic susceptibility of $S=1/2$ uniform AF Heisenberg chains (Bonner and Fisher 1964). (b) magnetic susceptibility of $S=1/2$ AF Heisenberg chains with the temperature-independent alternating J (Bonner *et al.* 1979). (c) magnetic susceptibility of the Haldane material abbreviated to NENP (Renard *et al.* 1987).
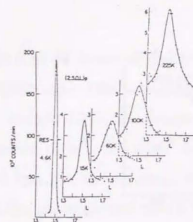
FIG. 3. Scans along $\vec{Q} = (2.5, 0, l)_r$ at a number of temperatures above and below the spin-dimerisation transition at $T_3 = 11$ K. A pronounced peak exists to temperatures as high as 225 K.

Fig. 3-3

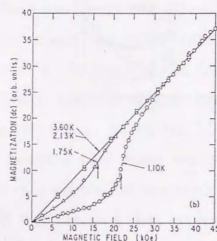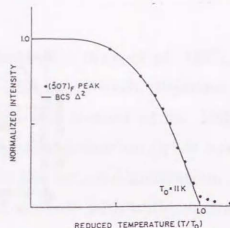X-ray diffraction pattern of TTF-CuBDT (Moncton *et al.* 1977).

FIG. 2. The temperature-dependent intensity of the new Bragg peaks which develop upon dimerization is accurately fitted by the BCS gap function.

Fig. 3-4

The temperature-dependent intensity of the new Bragg peak which develops upon the dimerization (Moncton *et al.* 1977).

Fig. 3-5

The magnetic-field dependence of the magnetization of TTF-AuBDT (Northby *et al.* 1982a).

Fig. 3-6

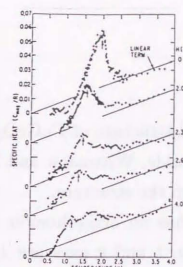The temperature dependence of the differential susceptibility of TTF-AuBDT (Northby *et al.* 1982a).

FIG. 3. Magnetic contributions to the specific heat in zero field and in various high fields $H \gtrsim H^*$ for TTF-BDTiAu. The arrows indicate the field-dependent cusplike anomaly [after Hijmans *et al.*, Ref. 13].

Fig. 3-7

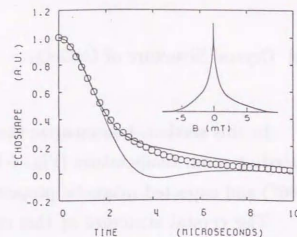The temperature dependence of the specific heat of TTF-AuBDT (Bonner *et al.* 1987).

FIG. 3. Real part of the Fourier transform (upper solid line) of the proton NMR line shape (inset) calculated for the soliton lattice with $R_{exp} = 0.1$, fitted to the experimental echo shape at $T = 0.75$ K and $B = 2.52$ T. The lower (thin) curve corresponds to a sinusoidal modulation.

Fig. 3-8

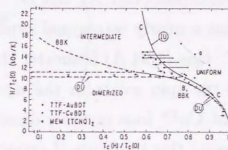The NMR line shape (Hijmans, Brom and de Jongh 1985).

FIG. 9. Composite normalized phase diagram for TTF-AuS$_4$C$_4$(CF$_3$)$_4$, TTF-CuS$_4$C$_4$(CF$_3$)$_4$, and (MEM-TCNQ)$_2$ powders. The normalized scales are $H/T_c(0)$ and $T_c(H)/T_c(0)$. Where possible, transitions are located by peak values of $(\partial M/\partial T)_H$ or $(\partial M/\partial H)_T$ (or χ_{ac}). For normalization, the values chosen for $T_c(0)$ are 2.03, 10.3, and 18.0 K for the compounds as listed. The line designated (a) represents mean-field estimates for the high-field phase boundary (for Cu) from data using a 10-MW solenoid ($H_{max} = 200$ kOe). The solid and dashed lines represent theoretical curves as in Fig. 3.

Fig. 3-9

The magnetic phase diagram of organic SP compounds (Northby *et al.* 1982a).

[4] Crystal Structure of CuGeO$_3$

In this section, I summarize the crystal structure of CuGeO$_3$ investigated at room temperature (Fig. 4-1; Völlenkle, Wittmann and Nowotny 1967) and expected magnetic properties from the structure.

The crystal structure of this cuprate has an orthorhombic unit cell (D_{2h}^5 - $Pbmm$). The lattice constants of a, b and c axes are 4.81, 8.48 and 2.94 Å, respectively. The Cu^{2+} ion has a $3d^9$ configuration and a $S=1/2$ spin. Other ions such as Ge^{4+} and O^{2-} have closed shells and are nonmagnetic. Each Cu^{2+} ion is crystallographically equivalent at room temperature. The distance between nearest neighbor Cu^{2+} ions, which are located along the c direction (2.94 Å), is much shorter than that between second nearest ones along the b direction (4.24 Å) and than that between third nearest ones along the a direction (4.81 Å). Six O^{2-} ions are located around Cu^{2+} ion and Cu site has a nearly tetragonal symmetry. Since the distance between Cu^{2+} and O$_2^{2-}$ ions (1.94 Å) is shorter than that between Cu^{2+} and O$_1^{2-}$ ions (2.78 Å), the spin exists in the $d_{x^2-y^2}$ orbit which extends into O$_2^{2-}$ ions. Adjacent Cu^{2+} ions in the c direction are coupled through two O^{2-} ions. Considering this structure, I expect a quasi-1D-AF interaction between spins on adjacent Cu^{2+} ions in the c direction. It is emphasized that the crystal structure of this cuprate is simpler than those of organic SP compounds.
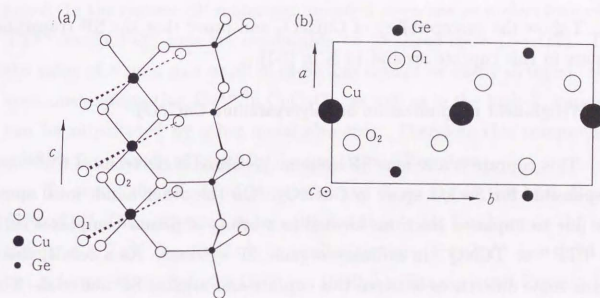

Fig. 4-1

The crystal structure of CuGeO$_3$.

22

23

[5] Purposes of the Present Studies

In this thesis, I report temperature (T) and magnetic field (H) dependences of magnetizations (M) of pure and Zn-doped $CuGeO_3$. The purposes of the present studies are summarized as follows.

[5-1] Magnetic susceptibility of single-crystal $CuGeO_3$

I show the susceptibility of $CuGeO_3$ and prove that the SP transition occurs in this cuprate around 14 K in [7-1].

[5-2] High-field magnetization of polycrystalline $CuGeO_3$

This cuprate is a unique SP system. Localized d electrons of Cu^{2+} are responsible for $S=1/2$ spins in $CuGeO_3$. On the other hand, local spins are due to unpaired electrons located in π orbits of planar complexes such as TTF^+ or $TCNQ^-$ in ordinary organic SP systems. As a result, there occur some differences between this cuprate and organic SP materials. For example, an average g-value of $CuGeO_3$ (2.18) (Petrakovskii *et al.* 1990) is larger than 2, which is considered to be due to the spin-orbit interaction of d electrons, while the g-value of organic SP compounds is nearly equal to 2 (TTF-CuBDT: Bray *et al.* 1975, TTF-AuBDT: Jacobs *et al.* 1976 and MEM-$(TCNQ)_2$: Huizinga *et al.* 1979). This difference may cause the material dependence of magnetic properties because the magnetization is finite in the M phase. Therefore it is important to examine whether the above-mentioned universality is valid for $CuGeO_3$ or not. Thus, we measured high-field magnetizations of this cuprate and compared our result with the known data of organic SP materials and the theories. The results will be described in [7-2].

[5-3] Magnetic susceptibility of polycrystalline $Cu_{1-x}Zn_xGeO_3$

The impurities doped in the antiferromagnetic (AF) quantum spin system significantly affect its physical properties. For example, Cu doped in the Haldane material causes the $S = 1/2$ degrees of freedom at the edges (Hagiwara *et al.* 1990), while Zn doped in the high-T_c cuprate drastically suppresses its superconductivity (Maeda *et al.* 1990). On the contrary, the effect of impurities for the spin-Peierls (SP) system has never been investigated. In the organic SP materials, unpaired electrons on molecules such as TTF^+ or $TCNQ^-$ ions are responsible for localized spins $(S=1/2)$. Thus the value of S on a part or all of these ions cannot be easily changed. However, one expects that Cu^{2+} in $CuGeO_3$, as well as in the high-T_c cuprates, can be substituted by other metal elements. Therefore this compound is suitable for a study of impurity doping in the SP system.

To study the effects of impurities, we chose Zn as the best dopant. First of all, Zn is expected to be substituted only for Cu, because the ionic radius of a Zn^{2+} ion (0.75 Å) is similar to that of a Cu^{2+} ion (0.73 Å), but is larger than that of a Ge^{4+} ion (0.40 Å) (Shannon and Prewitt 1969 and 1970). Secondly, the value of S on Cu sites will be unchanged, because both Cu and Zn cations are divalent. Thirdly, Zn^{2+} ions are nonmagnetic, that is, the magnetic susceptibility is mainly determined by the magnetic properties of Cu spins. The results will be described in [7-3].

[5-4] High-field magnetization of polycrystalline $Cu_{1-x}Zn_xGeO_3$

I report the high-field magnetizations of a series of $Cu_{1-x}Zn_xGeO_3$. Our main purposes are to study H, T and x dependences of the magnetizations especially in M phase and to examine whether the above-mentioned universality is valid for $Cu_{1-x}Zn_xGeO_3$ or not. The results will be described in [7-4].

[6] Experiments

[6-1] Sample preparations

I chose CuO (purity of 99.999 %), GeO_2 (purity of 99.9999 %) and ZnO (purity of 99.9 %) as starting materials. The single crystals of pure $CuGeO_3$ were grown by a self-flux method in air. A mixture of GeO_2 and CuO with a 1 : 1.2 molar ratio was melted in a platinum crucible around 1200 ℃ for about 24 hours and then was cooled slowly to 1100 ℃ for 50 hours. Obtained crystals were confirmed to be single-crystal $CuGeO_3$ by the x-ray diffraction pattern and Weissenberg method. The obtained single crystals are transparent with light-blue color and insulating. A typical dimension is about 0.05, 0.2 and 2 mm parallel to the a, b and c axes, respectively.

Fifteen samples of polycrystalline $Cu_{1-x}Zn_xGeO_3$ with x=0, 0.002, 0.005, 0.010, 0.020, 0.030, 0.035, 0.040, 0.045, 0.050, 0.060, 0.070, 0.080, 0.090 and 0.100 were prepared by an ordinary solid-state reaction method. They were sintered at about 1000 ℃ for about 50 hours in air. The x-ray diffraction patterns of the samples show that there are no trace of other impurity phases, and that the lattice constants are almost independent of x.

[6-2] Magnetization measurements

[6-2-1] SQUID magnetometer

The temperature dependence of the magnetic susceptibility was measured by an SHE model 905 SQUID magnetometer at our Laboratory and by a Quantum Design SQUID magnetometer at Electrotechnical Laboratory. The measured temperature and magnetic field are between $2 \sim 300$ K and between $0.01 \sim 5.5$ T, respectively.

[6-2-2] Induction method

Magnetization (M) was obtained as a function of H in pulsed magnetic fields up to 25 T with a duration time of about 12 ms at Institute for Solid State Physics, The University of Tokyo. The data of dM/dt and dH/dt were detected using an induction method and the values of M and H were numerically calculated. The pick-up coil of M consists of two coaxial coils wound in the opposite direction to cancel the voltage induced by the external magnetic field when a sample is removed. The length of the pick-up coil of M is about 7 mm. The inner coil with the radius of 2 mm has 400-turn windings, and the outer coil with the radius of 3 mm has 180-turn windings. The powder sample (about 137 mg) was stuffed into the inner coil. The pick-up coil of H is located near the pick-up coil of M. The measurement was performed at various temperatures from 3.5 to 20.3 K.

[6-2-3] Vibrating sample magnetometer

The magnetization was obtained as a function of H by the vibrating sample magnetometer in static H up to 15 T induced by a water-cooled magnet at Institute for Materials Research, Tohoku University. The measurement was performed at various temperatures from 2.0 to 15.0 K.

[6-2-4] Extraction-type magnetometer

The magnetization was obtained as a function of H by the extraction-type magnetometer in static H up to 23 T induced by a hybrid magnet at Institute for Materials Research, Tohoku University. The measurements were performed at various temperatures from 4.2 to 11.0 K.

[7] Results and Discussions

[7-1] Magnetic susceptibility of single-crystal CuGeO$_3$

The temperature dependence of the magnetic susceptibility of single-crystal CuGeO$_3$ is shown in Fig. 7-1 (Hase, Terasaki and Uchinokura 1993). Measurement was performed from 4.5 to 300 K under the magnetic field H of 1 T in the configurations with H parallel to three principal axes. The most striking feature is that the susceptibilities in all the directions $\chi_i(T)$ ($i = a, b$ and c) exponentially drop to small constant values below 14 K. The data measured in zero-field cooling and field cooling processes are identical. As usual we assume that the orbital part of the susceptibility χ_i^{orb} ($i = a, b$ and c) is independent of temperature, because it consists of Van Vleck paramagnetic susceptibility and diamagnetic one of core electrons. Although an accurate value of χ_i^{orb} is unknown, it is estimated to be of the order of 1×10^{-4} emu/mole, comparable with the magnitude of the 4.5-K susceptibilities. Since the spin parts of the susceptibilities $\chi_i^{spin}(T)$ ($i = a, b$ and c) can be obtained as $\chi_i^{spin}(T) = \chi_i(T) - \chi_i^{orb}$, the observed data strongly indicates that $\chi_i^{spin}(T)$ rapidly reduces to zero with decreasing temperature.

It is necessary to seek a possible origin of the rapid decrease of the susceptibility below 14 K. First of all, we emphasize that neither a 3D AF long-range order (LRO) nor a 1D Ising-like antiferromagnet (Bonner and Fisher 1964) can explain the observed data, because in these two cases the susceptibility decreases to zero as $T \to 0$ K only in one direction of the crystal and remains finite in other directions. Secondly, we also exclude a Haldane system because CuGeO$_3$ has linear spin chains with a half-integer spin of Cu^{2+}. (An integer-spin chain is essential to a Haldane system.)

Nonetheless the susceptibility of CuGeO$_3$ is very similar to that of Haldane materials, suggesting that the excitation spectrum of CuGeO$_3$ has a finite energy gap with a nonmagnetic ground state below 14 K.

There exists another system which shows a nonmagnetic ground state and a finite energy gap between the ground and excited states. It is a system of Heisenberg AF chains with alternating exchange interactions (Bulaevskii 1969). If the distance between $S = 1/2$ spins located on Cu^{2+} ions changes alternately, the AF exchange integral J will also change alternately. The susceptibility of this system is theoretically calculated and shows a rapid decrease slightly below a temperature at which the susceptibility is maximum (Bulaevskii 1969). As mentioned previously, positions of Cu^{2+} ions in CuGeO$_3$ are equivalent at room temperature (Völlenkle, Wittmann and Nowotny 1967), indicating that the AF interaction is uniform at room temperature. However, an abrupt change of the susceptibility at 14 K in Fig. 7-1 strongly suggests some kind of phase transition. This may cause the change of the homogeneous AF chain to an alternating AF chain.

To confirm existence of a phase transition at 14 K we have measured the specific heat (Fig. 7-2; Kuroe et al. 1994a). The experimental results clearly show an anomaly due to a second-order phase transition around 14 K. This definitely shows the existence of a phase transition at this temperature. Then there remain two possibilities. One is the case that a simple structural phase transition accidentally occurs with the doubling of the c length, which then induces the alternation of the AF couplings among the Cu^{2+} spins. The other is a spin-Peierls transition, which has been confirmed to exist only in organic compounds. The difference between the two is whether the AF interaction is essential to the phase transition or not.

Before reaching a conclusion let us discuss the magnetic properties above the transition temperature. The temperature dependence of the

susceptibilities in the a, b and c axes shown in Fig. 7-1 is almost identical with one another except for a weak anisotropy. The spin parts of the susceptibilities $\chi_i^{spin}(T)$ can be obtained as discussed before. The ratios $\chi_a^{spin}(T)/\chi_c^{spin}(T)$ and $\chi_b^{spin}(T)/\chi_c^{spin}(T)$ are 1.10 and 1.22, respectively, in the temperature region between 4.5 and 300 K. This suggests that the magnetism of this compound can be described by a Heisenberg model,

$$H = J \sum_{<i,j>} \mathbf{S}_i \cdot \mathbf{S}_j. \qquad (7-1)$$

The susceptibility has a broad maximum near 56 K and slowly decreases above 56 K with increasing temperature. This broad maximum strongly indicates the existence of an AF exchange interaction (Bonner and Fisher 1964). As was discussed already, a magnetic interaction of the spins in $CuGeO_3$ is expected to be 1D. The value of J is calculated to be about 88 K according to the model of uniform Heisenberg AF linear chains (Bonner and Fisher 1964). However, as is seen in Fig. 7-1(a), the experimental results does not quantitatively agree with the theory. The magnitude of the former is smaller than that of the latter, and the temperature dependence of the former is weaker than that of the latter. We cannot at present determine the reason of this discrepancy but the weak interchain coupling between the spins or the temperature dependence of the exchange interaction may be possible reasons. The discrepancy between the measured susceptibility above the transition temperature and the theories must be studied in more detail.

We will prove that the phase transition of $CuGeO_3$ is really the spin-Peierls transition. In Fig. 7-3 we show the temperature dependence of the susceptibility of a polycrystalline sample under various magnetic fields. It can be seen that the transition temperature shifts to lower temperature with increasing magnetic field. We cannot expect the shift of the transition
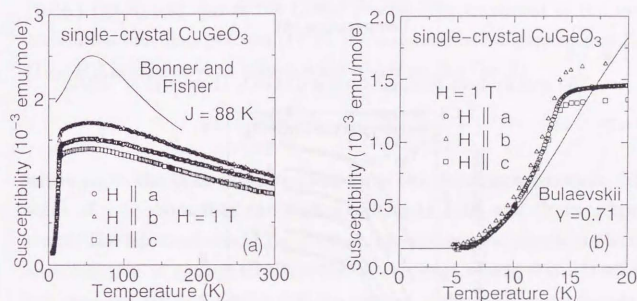

Fig. 7-1

The magnetic susceptibility of single-crystal $CuGeO_3$ measured in $H = 1$ T (Hase, Terasaki and Uchinokura 1993). (a) The susceptibility from 4.5 to 300 K. The solid curve is a theoretical one calculated by Bonner and Fisher (1964) with $J=88$ K. (b) The susceptibility below 20 K. The solid curve is a theoretical one calculated by L. N. Bulaevskii (1969). The value of J and the ratio between two alternating J's (γ) are 103 [$=88(1+0.17)$] K and 0.71, respectively, which are estimated in the text. The value of χ_i^{orb} is assumed to be 1.5×10^{-4} emu/mole.
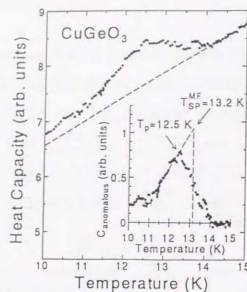
Fig. 7-2

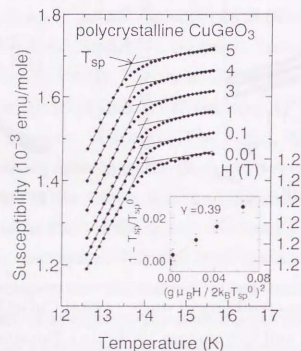The specific heat of single-crystal $CuGeO_3$ (Kuroe *et al.* 1994a).

Fig. 7-3

The magnetic susceptibility of polycrystalline $CuGeO_3$ measured near the phase transition temperature, $T_{SP}(H)$, in $H = 0.01 \sim 5$ T. As is seen in this figure, each value of $T_{SP}(H)$ is defined as the temperature of the intersection of two lines along each curve. The vertical position of each data is shifted as indicated on the right-hand side of the figure. Inset: $1 - \frac{T_{SP}(H)}{T_{SP}(0)}$ vs $\left(\frac{g\mu_B H}{2k_B T_{SP}(0)}\right)^2$.

temperature to lower temperature in a simple structural phase transition. Therefore the possibility of a simple structural phase transition can be excluded in $CuGeO_3$ and it is concluded that the spin-Peierls transition occurs around 14 K.

Now let us compare the experimental results with theories and the experimental results of the already known organic spin-Peierls systems. According to the Hartree-Fock theory of Bulaevskii, Buzdin and Khomskii (BBK) (1978) and also to the Luther-Peschel-type treatment of the spin-correlation functions of Cross (1979), the magnetic field dependence of T_{SP} [$T_{SP}(H)$] is expressed as follows when $g\mu_B H \ll 2k_B T_{SP}(0)$,

$$1 - \frac{T_{SP}(H)}{T_{SP}(0)} \sim \gamma \left(\frac{g\mu_B H}{2k_B T_{SP}(0)}\right)^2, \qquad (7-2)$$

where μ_B is the Bohr magneton and k_B is the Boltzmann constant. The value of γ is about 0.44 and 0.38 according to BBK and Cross, respectively. The left-hand side of Eq. (7-2) of the experimental results is plotted as a function of $(g\mu_B H/2k_B T_{SP}(0))^2$ in the inset of Fig. 7-3. It shows the expected H^2 dependence and the value of γ obtained in our sample is about 0.39, which is in excellent agreement with 0.38 of Cross (1979). This means that the Luther-Peschel-type treatment (Luther and Peschel 1975) of Cross and Fisher (1979) and the phase Hamiltonian method of Nakano and Fukuyama (1980 and 1981), which properly took into account the Umklapp effects in zero magnetic field, give more suitable ground for understanding the spin-Peierls transition in the magnetic field than the Hartree-Fock treatment, on which the papers of Bray J. W. 1978 and Bulaevskii, Buzdin and Khomskii 1978 are based. In organic spin-Peierls systems it has been established that the phase boundaries are expressed by a universal phase diagram (Northby *et al.* 1982a), which in particular at low magnetic-field range coincides with the theories of BBK as well as Cross. This means

that the phase boundary between the spin-Peierls and the uniform states in CuGeO$_3$ agrees with that of the organic spin-Peierls systems.

Below T_{SP} two alternating J's $[J_{1,2}(T)]$ are formed and expressed as follows (Pytte 1974);

$$J_{1,2}(T) = J\{1 \pm \delta(T)\}. \qquad (7-3)$$

According to the mean-field theory of Pytte the relationship between $\delta(T)$ and the excitation energy gap $\Delta(T)$ at temperature T is expressed as (Bray et al. 1975)

$$\delta(T) = \frac{\Delta(T)}{pJ}, \qquad (7-4)$$

where the value of p is 1.637. Bulaevskii has calculated the susceptibility of the system of the Heisenberg AF linear chains with temperature-independent alternating J in the Hartree-Fock approximation (Bulaevskii 1969). The value of $\delta(T)$ and therefore $\Delta(T)$ can be obtained by combining the Bulaevskii's theory with Eqs. (7-3) and (7-4). By this method we obtained $\delta(0) = 0.17$, (i.e., $J_2(0)/J_1(0) = 0.71$) and $\Delta(0) = 24$ K. These values are isotropic, because $\chi_i^{spin}(T)$'s are almost identical if they are normalized by their maximum values as was discussed before. It should be noted that the experimental data cannot be simply explained by the model of the Heisenberg AF linear chains with temperature-independent alternating J. In Fig. 7-1(b), we show a theoretical curve of this model with estimated parameters. The discrepancy between the theoretical curve and the experimental data becomes evident above 10 K, which is due to a temperature dependence of $J_{1,2}(T)$. The value of $\frac{2\Delta(0)}{k_B T_{SP}}$ is 3.43, which is close to the values of organic spin-Peierls materials (3.53, 3.7, and 3.16 for TTF-CuBDT (Bray et al. 1975), TTF-AuBDT (Jacobs et al. 1976) and MEM-(TCNQ)$_2$ (Huizinga et al. 1979), respectively). According to the

theory of Cross and Fisher (1979), T_{SP} is given by

$$T_{SP} = 0.8J\eta', \qquad (7-5)$$

where η' is the spin-lattice coupling constant. From Eq. (7-5) we obtain $\eta' = 0.20$. The values of η' and $\Delta(0)$ in CuGeO$_3$ are surprisingly close to those of TTF-CuBDT (0.18: Bray et al. 1975) or MEM-(TCNQ)$_2$ (0.21: Huizinga et al. 1979).

The properties of CuGeO$_3$ can be well described by the existing theories of spin-Peierls transition and no inconsistencies with the theories have been found. Moreover the agreement with the experimental results in organic spin-Peierls systems is very good. I think that they have firmly proven the existence of spin-Peierls transition in Cu^{2+} linear chains in an inorganic compound CuGeO$_3$.

In the following paragraphs, I report further investigations of CuGeO$_3$ such as the neutron scattering measurements (Nishi, Fujita and Akimitsu 1993), the X-ray structural analyses (Izumi et al. 1993), the nuclear quadrupole resonance (NQR) (Kikuchi et al. 1994), the Raman scattering spectra (Kuroe et al. 1994b, and Sugai 1993a and 1993b) and the optical reflectivity spectra (Terasaki et al. 1994). From these studies, the following results have been obtained at present.

(1) The phase transition occurs around 14 K, and the ground state is nonmagnetic and the finite magnetic energy gap opens below 14 K. These properties are consistent with the result of our works.

(2) A static lattice distortion has not been observed so far. This does not agree with those expected for the SP transition.

(3) The exchange interaction is quasi-1D in CuGeO$_3$. However the interchain exchange interaction in the direction of b axis is not so small.

In the inelastic neutron scattering measurements, the intensity with the energy transfer $\Delta E = 1$ meV at (0,1,0.5) decreases exponentially below

14 K due to the SP gap formation [Fig. 7-4(a); Nishi, Fujita and Akimitsu 1993]. From the data of the dispersion curve [Fig. 7-4(b); Nishi, Fujita and Akimitsu 1993], the energy gap around 0 K was derived to be about 2.11 meV (24.5 K), which agrees with the estimated value by us (24 K). The value of the exchange interaction along the c axis (J_c) is about 10.4 meV (AF), and those along the b and a axes are about $0.1J_c$ (AF) and $-0.01J_c$ (ferromagnetic), respectively. Although these results are consistent with the appearance of the SP transition, a satellite peak due to a lattice dimerization has not been found so far. There are also no evident observations of a new peak in the X-ray measurements (Izumi *et al.* 1993).

The following results were obtained in the NQR measurements (Kikuchi *et al.* 1994). The NQR signals persist down to 1.3 K with neither line splitting nor broadening due to an internal field. This fact means that there is no long range order (LRO) of Cu spins down to 1.3 K. The ^{63}Cu nuclear spin-lattice relaxation rate $^{63}(1/T_1)$ rapidly drops below about 14 K, which indicates the opening of the energy gap (Fig. 7-5). An extrapolated value of $^{63}(1/T_1)$ to 0 K is finite. This result indicates that a magnetic LRO does not exist even at 0 K, and that the exchange interaction is a 1D Heisenberg type. On the other hand, the NQR frequency (ν_{NQR}) is almost T-independent from 4.2 to 20.0 K (Fig. 7-6). It is noted that a change of ν_{NQR} has not been detected at T_{SP}.

In the above-mentioned investigations, a change at T_{SP} has not been observed except for the magnetic properties. On the other hand, new peaks appear below T_{SP} in the Raman scattering spectra (Kuroe *et al.* 1994b, and Sugai 1993a and 1993b). However the origin of these new peaks is not known. I emphasize that the optical reflectivity spectra is nearly T-independent (Terasaki *et al.* 1994).
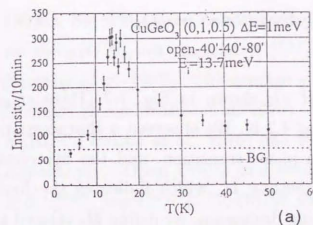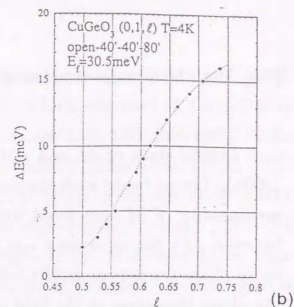

Fig. 7-4

The neutron scattering measurements of single-crystal CuGeO₃ (Nishi, Fujita and Akimitsu 1993). (a) the temperature dependence of the neutron scattering intensity at $\Delta E = 1$ meV. (b) the dispersion relation of the magnetic exciton along the c axis.
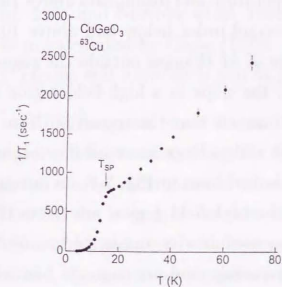

Fig. 7-5

The temperature dependence of the ^{63}Cu nuclear spin-lattice relaxation rate $^{63}(1/T_1)$ (Kikuchi *et al.* 1994).

Fig. 7-6
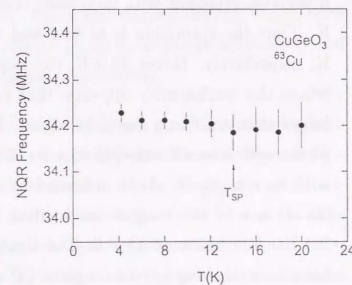
The temperature dependence of the NQR frequency (ν_{NQR}) (Kikuchi *et al.* 1994).

[7-2] High-field magnetization of polycrystalline CuGeO$_3$

Typical data of M and dM/dH are shown in Fig. 7-7 (Hase *et al.* 1993a). Let us begin with the data at 4.2 K. We observed a characteristic nonlinearity of M associated with a phase transition, and the hysteresis between M's for increasing and decreasing H, which indicates the first-order phase transition. In the following discussion, we define H_c related to the phase transition as the field of the peak position in the dM/dH curve, which is indicated by triangles in Fig. 7-7. The value of H_c measured in increasing field (H_c^{up}) is slightly larger than that measured in decreasing field (H_c^{down}). As temperature is raised, the nonlinearity becomes less evident till 13.4 K, and M is a linear function of H up to 25 T above 13.8 K. The hysteresis decreases with increasing temperature and disappears above 10.0 K. Thus the transition is of first and second order below and above 10.0 K, respectively. Below 13.8 K, the slope of M changes outside the region where the nonlinearity appears, that is, the slope in a high-field region is larger than that in a low-field region. It means that the transition from a phase with a small susceptibility to that with a large susceptibility occurs with increasing H. As is indicated by dashed lines in Fig. 7-7, an extrapolated line of the magnetization from the high-field region intersects the left-hand ordinate at $M \sim 0$. The similar nonlinearity and hysteresis of M have been also reported in organic SP materials, and are common features of the SP system (Bray *et al.* 1979, Bloch *et al.* 1980, Bloch *et al.* 1981 and Northby *et al.* 1982a). The magnetization was also measured in static magnetic fields (Fig. 7-8). The T dependence of the magnetization is weak in a high-H region.

We show the magnetic phase diagram expressed in terms of the reduced variables h [$=gH/2T_{SP}(0)$] and t [$=T/T_{SP}(0)$] in Fig. 7-9 (Hase *et al.*

1993a). Since the Zeeman energy depends on the g-value as well as H itself, we use $gH/2T_{SP}(0)$ instead of $H/T_{SP}(0)$, which was used in the paper of Northby *et al.* 1982a. The average g-values are 2.18, 1.97, 2.05 and 2.00 for CuGeO$_3$ (Petrakovskii *et al.* 1990), TTF-CuBDT (Bray *et al.* 1975), TTF-AuBDT (Jacobs *et al.* 1976) and MEM(TCNQ)$_2$ (Huizinga *et al.* 1979), respectively. Open circles and triangles represent h_c^{up} [$=gH_c^{up}/2T_{SP}(0)$] and h_c^{down} [$=gH_c^{down}/2T_{SP}(0)$] in the region of the first-order phase transition, respectively, and closed squares h_c [$=gH_c/2T_{SP}(0)$] in the region of the second-order phase transition. Closed diamonds represent the magnetic field dependence of T_{SP} [$T_{SP}(H)$] determined from $\chi(T)$'s, which were measured in constant fields up to 5 T by a SQUID magnetometer in our previous work (Hase, Terasaki and Uchinokura 1993). The data of typical organic SP materials are also included in this figure (Bloch *et al.* 1980, Bloch *et al.* 1981 and Northby *et al.* 1982a). Solid and dashed curves, which have been calculated by Cross (1979), denote phase boundaries between D and U phases and between U and M phases, respectively.

The magnetic phase diagram of CuGeO$_3$ agrees qualitatively with both experimental results of organic SP systems and the theoretical prediction despite large differences in crystal structures. As a result, we could determine the boundary between D and the other phases in this work. The value of h_c decreases with increasing temperature above $t \sim 0.74$. In other words, the transition temperature is decreased by the field. The reduction of the transition temperature is due to the suppression of spin fluctuation and the increasing Zeeman energy. Especially below $h \sim 0.39$ ($H \sim 5$ T), the data of CuGeO$_3$ and theoretical curve exhibit an excellent agreement. On the other hand, below $t \sim 0.74$, the value of h_c^{up} is nearly independent of temperature and that of h_c^{down} decreases slightly as temperature is lowered (The value of H_c is 12~13 T). The difference between the values of

h_c^{up} and h_c^{down} increases with decreasing temperature, which qualitatively agrees with the results of organic SP materials. The existence of the first-order phase transition is theoretically suggested in the following papers; Nakano and Fukuyama 1980 and 1981, Inagaki and Fukuyama 1984 and Harada and Kotani 1982.

The phase boundary between the U and M phases was determined in the differential susceptibilities (Fig. 10; Hamamoto *et al.* 1994) and is consistent with both experimental results of organic SP systems and the theoretical prediction. Recently the first analysis of the line shape in the electron spin resonance (ESR) has been done in a high-H region (Adachi *et al.* 1994). The line shape at 78 K in the U phase obeys Lorentzian, which indicates the existence of an exchange narrowing. On the other hand, the line shape at 5 K in the M phase obeys Gaussian, which indicates the existence of an incommensurate structure.

In the following paragraphs, we discuss the material dependence of the magnetic phase diagram, which is observed in the transition region between D and M phases. The value of h_c indicating the DM transition (h_c^{DM}) varies in all the compounds, which had been considered to be almost the same (Northby *et al.* 1982a). The difference between the values of h_c^{up} and h_c^{down} in CuGeO$_3$ is smaller than that in TTF-CuBDT (Bloch *et al.* 1980) or MEM(TCNQ)$_2$ (Bloch *et al.* 1981). The value of t below which the transition is of first order is about 0.71 in CuGeO$_3$, which is close to the value obtained in MEM(TCNQ)$_2$ (0.67) and slightly larger than the values obtained in TTF-CuBDT and TTF-AuBDT (Hijmans, Brom and de Jongh 1985) (0.50 and 0.50, respectively).

It is commonly considered that the interchain exchange interaction affects the properties of the M phase, because the magnetization is finite in the M phase. Inagaki and Fukuyama (1984) have obtained the phase

diagram at 0 K in the presence of the magnetic field for the quasi-one-dimensional Heisenberg antiferromagnet coupled with the lattice distortion. According to their theory, the value of h_c^{DM} is lowered by the existence of the interchain exchange interaction. I think that the small variation of h_c^{DM} in SP materials is caused by the interchain exchange interaction, which may depend on crystal structures.
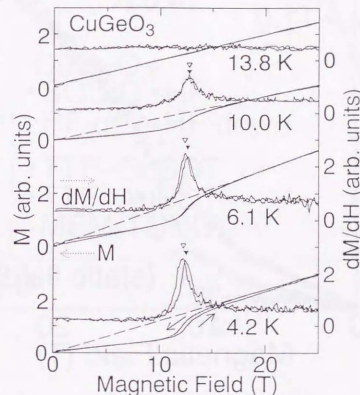
The magnetic-field dependence of M and dM/dH of polycrystalline CuGeO$_3$ at 4.2, 6.1, 10.0 and 13.8 K in pulsed magnetic fields (Hase *et al.* 1993a). The vertical positions of M and dM/dH are shifted as indicated on the left-hand and right-hand sides of the figure, respectively. Closed and open triangles denote the peak position of dM/dH measured in increasing and decreasing fields, respectively. Solid arrows represent the directions of the scan of the field. Dashed lines mean the extrapolation of the magnetization from the high-field region to $H=0$.
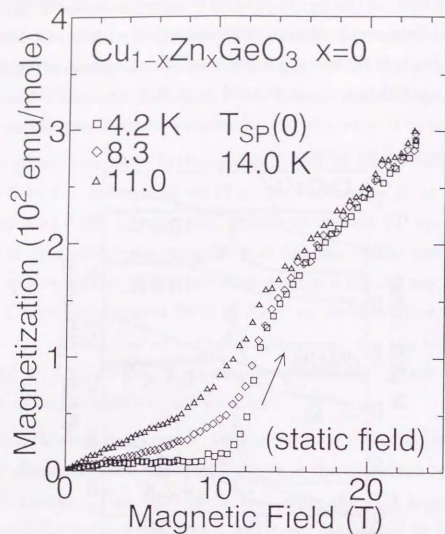
Fig. 7-8

The magnetic-field dependence of M of polycrystalline $CuGeO_3$ at 4.2. 8.3 and 11.0 K in static magnetic fields. Solid arrows represent the directions of the scan of the field.

Fig. 7-9
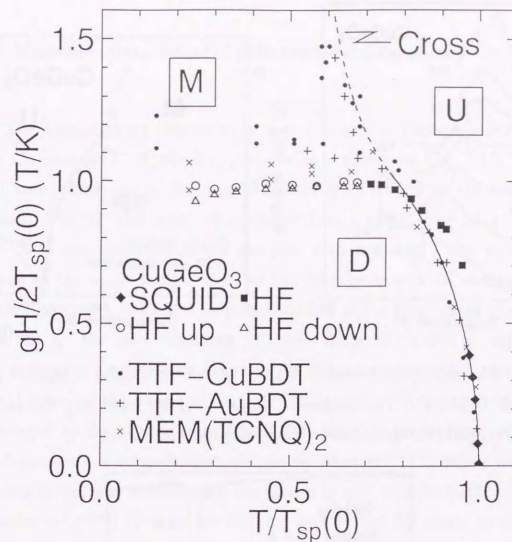
The magnetic phase diagram of $CuGeO_3$ (Hase et al. 1993a). Open circles. open triangles and closed squares represent the critical fields determined from the magnetizations measured in the high-magnetic fields up to 25 T. and closed diamonds spin-Peierls transition temperature derived from the susceptibilities measured by a SQUID magnetometer. This figure includes the data of typical organic spin-Peierls materials. Solid and dashed curves are theoretical ones. D. U and M denote dimerized. uniform and magnetic phases, respectively. References: TTF-CuBDT from Bloch et al. 1980. TTF-AuBDT from Northby et al. 1982a. MEM(TCNQ)$_2$ from Bloch et al. 1981 and theoretical curves from Cross 1979.
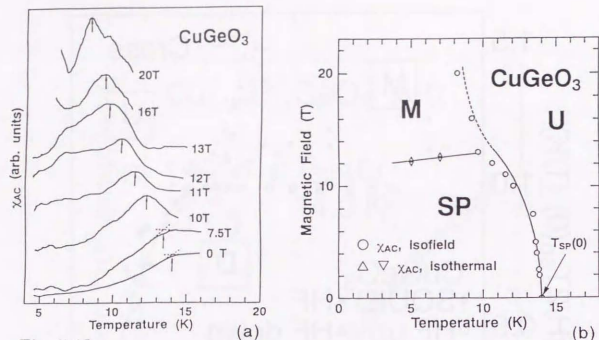
Fig. 7-10

(a) The differential susceptibilities of polycrystalline $CuGeO_3$ in high magnetic fields; (b) The magnetic phase diagram including the results of the differential susceptibilities (Hamamoto *et al.* 1994).
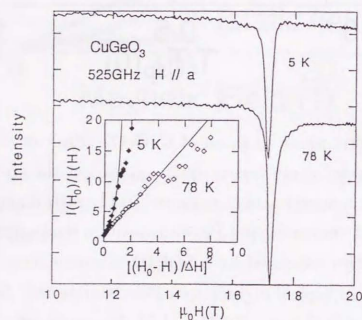
Fig. 7-11

The ESR measurements in the far infrared region of $CuGeO_3$ (Adachi *et al.* 1994).

[7-3] Magnetic susceptibility of polycrystalline $Cu_{1-x}Zn_xGeO_3$

The temperature dependence of the magnetic susceptibility per one-mole Cu ions [$\chi(T,x)$] of $Cu_{1-x}Zn_xGeO_3$ is shown in Fig. 7-12. Measurement was performed in the magnetic field H of 0.01 T in the field-cooling process. The SP transition characterized by a rapid drop of $\chi(T,x)$ near $10 \sim 14$ K was observed in the samples with $x \leq 0.02$. The value of T_{SP} defined as the onset temperature of the drop reduces with doping and disappears around $x = 0.03$. The magnitude of $\chi(T,x)$ increases upon doping below 20 K. We also measured $\chi(T,x)$'s from 20 to 300 K, which show only a weak x dependence (Fig. 7-13). This suggests that the spin and orbital parts of the susceptibility [$\chi^{spin}(T)$ and χ^{orb}, respectively] remain unchanged by Zn doping from 20 to 300 K. Since in general the value of χ^{orb} is independent of temperature, we can see that $\chi^{spin}(T)$ below about 20 K drastically changes with doping. As is seen in $\chi(T,x)$'s for $0.002 \leq x \leq 0.02$, the value of $\chi^{spin}(T)$ does not become zero in the SP state, in contrast to that of $x = 0$. These finite $\chi^{spin}(T)$'s are mainly caused by spins which do not become singlet because of the existence of Zn ions.

Most unexpectedly, we discovered an occurrence of another phase transition characterized by a cusp of $\chi(T,x)$ around $2 \sim 5$ K for $0.02 \leq x \leq 0.08$. We emphasize that the sample with $x = 0.02$ has two phase transitions. On the other hand, the $\chi(T,x)$'s for $x = 0.09$ and 0.10 monotonically increase as temperature is lowered below 20 K and show no transitions. In order to see the novel phase transition more clearly, the data for $x = 0.04$ measured in various H's below 5 K is shown in Fig. 7-14 (Hase *et al.* 1993b). A remarkable hysteresis is observed between the zero-field-cooling (ZFC) and field-cooling (FC) processes in the data in 0.01 T below 4.7 K. The transition temperature is defined as the temperature at which the irreversibility

begins, and is slightly higher than the temperature at which the susceptibility has the cusp. As the magnetic field increases, the hysteresis becomes less evident and the susceptibility reduces both below and above the transition temperature at low temperatures. The above-mentioned properties of the susceptibility strongly indicate that a spin-glass-like (SG-like) phase transition (Binder and Young 1986) occurs in $Cu_{1-x}Zn_xGeO_3$ for $0.02 \leq x \leq 0.08$. However, the ZFC susceptibility of $Cu_{1-x}Zn_xGeO_3$ is different from that of an ordinary spin-glass material which monotonically diminishes with decreasing temperature below the transition temperature. We cannot at present determine the reason of this difference. This SG-like transition has characteristic properties, that is, a small amount of impurities causes the phase transition and the SG-like transition temperature (T_{SG}) is much smaller than J_{intra}. Analogous results were obtained in other quasi-one-dimensional magnetic systems. For example, an anomaly was observed around 3 K in the magnetic susceptibility of $CsCo_{1-x}M_xCl_3$ [M=Mg or Zn: $x \sim 0.01$, $J_{intra} \sim 75$ K (AF)], and interpreted by the random field (Fig. 7-15; Mekata et al. 1987). The SG-like transition was seen around 1.8 K in the differential susceptibility of $C_6H_{11}NH_3Cu_{1-x}Mn_xCl_3$ [$x = 0.009$, $J_{intra} \sim -70$ K (ferromagnetic)] (Fig. 7-16; Cheikhrouhou, Dupas and Renard 1983). In these materials, the interchain exchange interaction is considered to play an important role in the occurrence of the random field or SG-like transition. On the other hand, a Haldane material with impurities shows neither a phase transition nor an anomaly. It should be emphasized that the value of $|J_{inter}/J_{intra}|$ (J_{inter} is the value of the interchain exchange interaction) is very small ($\sim 10^{-4}$) in the Haldane material (Renard et al. 1987).

The x dependences of T_{SP} [$T_{SP}(x)$] and T_{SG} [$T_{SG}(x)$] are shown in Fig. 7-17. The value of $T_{SP}(x)/T_{SP}(0)$ linearly reduces up to $x \leq 0.02$,

which is expressed as $1 - 13.7x$, and the SP state collapses around $x = 0.03$. This means that the value of T_{SP} drastically decreases by a small amount of Zn doping. For example, as is shown in Fig. 7-18 (Cheong et al. 1991), the decrease of the Néel temperature [$T_N(x)$] caused by the magnetic dilution is expressed as follows; $T_N(x)/T_N(0) = 1 - \alpha x$, ($\alpha \sim 1$ in two or three-dimensional magnetic systems). On the other hand, the SG-like transition is seen in the samples with $0.02 \leq x \leq 0.08$, and the value of $T_{SG}(x)$ has a maximum around $x = 0.04$.

We point out that $\chi(T, x)$'s at low temperatures do not obey a simple Curie law. The data of $\log_{10}[\chi(T, x)]$ vs. $\log_{10}(T)$ is shown in Fig. 7-19 (Hase et al. 1993b). The divergence of $\chi(T, x)$'s is weaker than $1/T$ in each data. The slope of the curve changes outside the region where the SG-like transition occurs, that is, the slope for $x \leq 0.01$ is larger than that for $x = 0.10$. Bulaevskii (1969) has calculated the susceptibility of the uniform AF Heisenberg linear chain with defects, which diverges as $1/T$. On the other hand, Bulaevskii et al. (1972) have also calculated the susceptibility of the one-dimensional (1D) system with a distributed AF interaction, which diverges weaklier than $1/T$. These theories strongly suggest that the AF interaction is not uniform at low temperatures in all the samples. The nonuniformity may come from a local lattice distortion and/or a disorder of AF interactions in these samples, although the SP transition is not observed in the samples with $0.03 \leq x \leq 0.10$. We point out as another feature of the divergent term that the total amount of spins contributing to it increases with x. Suppose that $\chi(T, x)$ is roughly expressed as $C(x)T^{-\gamma(x)}$ [$\gamma(x) < 1$] at low temperatures. To explain the increase of the magnitude of $\chi(T, x)$ with x, we conclude that only the value of $C(x)$ increases with x, because the slope, $\gamma(x)$, is nearly constant or slightly decreases with x. The value of $C(x)$ is in general proportional to the total amount of spins,

although an exact expression depends on a theoretical model. As is above-mentioned, the strong x dependence was observed in $\chi(T, x)$'s below 20 K, which indicates that Zn homogeneously distributes in the AF chains in each sample.

To discuss the effects of impurities on the SP transition, let us remind the theories of this transition, which were given in [2]. The Hamiltonian for the SP system is changed into that expressed in terms of spinless-fermion operators by the Jordan-Wigner (1928) and Fourier transformations. To treat the SP transition properly, it is necessary to include the interactions between spinless fermions accurately. Cross and Fisher (1979) have developed a theory of the SP transition with using boson representations of fermion operators. Nakano and Fukuyama (1980 and 1981) have obtained a phase Hamiltonian, and succeeded in treating properly the ground state and the low-lying excitations in the SP state. According to the theory of Cross and Fisher, the value of T_{SP} is determined from the following equations; $0 = \Omega_0^2(2k_F) + \Pi(2k_F, T_{SP})$ and $\Pi(2k_F, T) = -1.04|g(2k_F)|^2 T^{-1}$, where $\Omega_0(q)$, $\Pi(q, T)$, $g(q)$ and k_F denote the phonon frequency in the absence of the spin interactions, the polarizability, the coupling constant between the 1D spin and three-dimensional phonon systems, and the Fermi wave vector, respectively.

Let us consider the SP transition in $Cu_{1-x}Zn_xGeO_3$. The rapid and linear decrease of T_{SP} reminds us of the reduction of the Peierls transition temperature (T_P) in a low-dimensional conductor with nonmagnetic impurities (Roshen 1985), e.g., $Ta_{1-x}Nb_xS_3$ [$T_P(x)/T_P(0) \sim 1 - 31.3x$: $T_P(x)$ is T_P for x.] (Fig. 7-20; Hsieh P.-L. 1983). The Hamiltonian for the SP system expressed by spinless fermions is nearly equivalent to that for the Peierls system except for the interaction terms among spinless fermions. Thus we think that the reduction of T_{SP} originates from the disorder of the

spinless-fermion band induced by Zn ions. Although an explicit expression of the polarizability in $Cu_{1-x}Zn_xGeO_3$ has not been obtained, it is considered that the absolute value of the polarizability becomes smaller upon Zn doping at the same temperature because of the disorder of the spinless-fermion band. Since the SP transition occurs at the temperature where the value of $-\Pi(2k_F, T)$ is equal to that of $\Omega_0^2(2k_F)$, the value of T_{SP} reduces with doping. Further investigations are necessary for the quantitative understanding of the reduction of T_{SP} both experimentally and theoretically. In the theoretical aspect, Lu, Su and Yu (1993) recently have studied the effects of doping on SP systems using the unimodular mean-field theory and have obtained the result that T_{SP} and the energy gap are reduced. The calculated value of $T_{SP}(x)$ quantitatively agrees with the experimental data.

We shall have a closer look at the newly discovered SG-like transition. As is seen above, the SP order is destroyed by Zn. The disappearance of the SP order leads to a development of the 1D AF correlation in each chain, which is considered to play an important role in the appearance of the SG-like transition. However, in addition to the 1D AF correlation, some other conditions are necessary for the occurrence of the SG-like transition; the frustration and/or randomness in the exchange interaction (Binder and Young 1986). There is randomness, because Zn is randomly distributed in chains. However, it is not a simple problem whether there is frustration or not. If the chain is strictly 1D, the frustration does not exist. On the other hand, a spin-glass transition occurs in a magnet, where the exchange interaction is 2D or 3D (e.g., 2D-AF Kagomé lattice (Ramirez, Espinosa and Cooper 1990)). Then we consider the following scenario. Even in a pure SP system, there should be a weak interchain exchange interaction at least in a paramagnetic state, which does not affect the SP state because most of

spins are singlet below T_{SP}. As a result, the 2D or 3D magnetic correlation exists and may produce frustration. We think that the interchain exchange interaction is necessary for the occurrence of the SG-like transition.

We consider the x dependence of the 2D or 3D magnetic correlation. The energy of the 2D or 3D magnetic correlation and then T_{SG} are roughly estimated to be proportional to $|\xi_\| J_{inter}|$ where $\xi_\|$ is the 1D AF correlation length in the chain. The value of $\xi_\|$ is proportional to T^{-1} in general (Luther and Peschel 1975), while that of J_{inter} is almost independent of T. Therefore a phase transition may occur when the magnetic energy, which increases with decreasing temperature, coincides with the thermal energy. The Zn doping hardly changes the value of J_{inter} dominated mainly by the interchain exchange interaction inherent in the undoped system, whereas the Zn doping changes $\xi_\|$. In the small x region, the value of $\xi_\|$ increases upon Zn doping because of the reduction of the SP order and the corresponding development of the 1D AF correlation. As a result, the value of $T_{SG}(x)$ increases. On the other hand, in the large x region, the value of $\xi_\|$ is limited to an average distance between two neighboring Zn ions in chains, because the two Cu spins located on opposite sides of Zn within a chain interact weaklier than the two neighboring Cu spins within a chain. Since the average distance between two neighboring Zn ions in chains reduces with doping, the values of $\xi_\|$ and T_{SG} decrease. In order to understand the SG-like state and microscopic state of chains in more detail, more experiments, such as the differential susceptibility and electron nuclear double resonance, are needed.
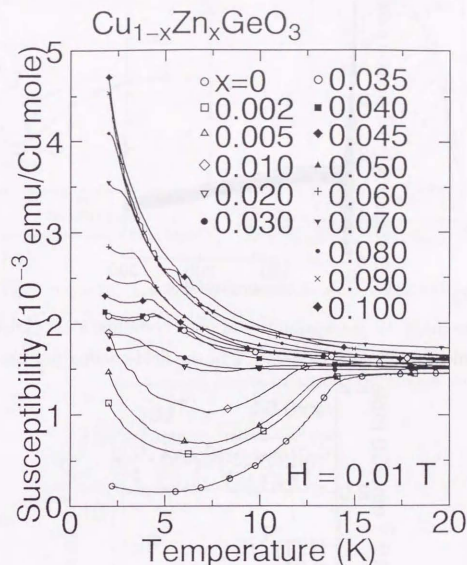
Fig. 7-12

The magnetic susceptibilities of polycrystalline $Cu_{1-x}Zn_xGeO_3$ below 20 K measured under $H = 0.01$ T in the field-cooling process. We measured the data at an interval of 0.2 K in general. Many experimental points have been suppressed in order to improve the clarity of the figure. The susceptibility for $x = 0$ was derived from that of single-crystal $CuGeO_3$ measured under $H = 1$ T, because polycrystalline $CuGeO_3$ includes a small amount of divergent term.
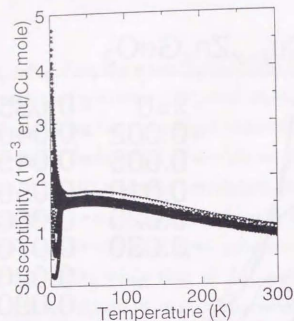
Fig. 7-13

The magnetic susceptibilities of polycrystalline $Cu_{1-x}Zn_xGeO_3$ below 300 K measured under $H = 0.01$ T in the field-cooling process.
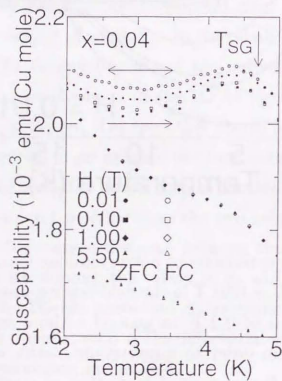
Fig. 7-14

The magnetic susceptibility of the sample with $x = 0.04$ below 5 K measured in various H's (Hase et al. 1993b). ZFC and FC indicate the zero-field-cooling and field-cooling processes, respectively. Horizontal solid arrows mean the directions of the temperature scan.
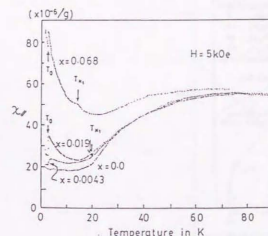

Fig. 3. Thermomagnetic curves of $CsCo_{1-x}Mg_xCl_3$.

Fig. 7-15

The magnetic susceptibility of $CsCo_{1-x}Mg_xCl_3$ (Mekata et al. 1987).
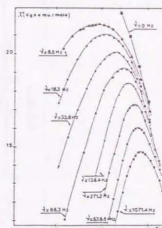
Fig. 7-16

The differential susceptibility of $C_6H_{11}NH_3Cu_{0.991}Mn_{0.009}Cl_3$ (Cheikhrouhou, Dupas and Renard 1983).
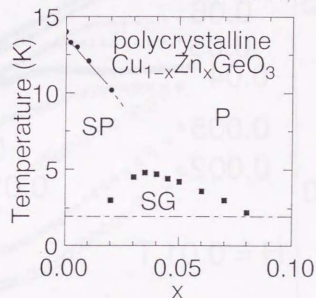
Fig. 7-17

The x dependences of $T_{SP}(x)$ (closed circles) and $T_{SG}(x)$ (closed squares). Spin-glass-like, spin-Peierls and paramagnetic states are abbreviated to SG, SP and P, respectively. The dotted-dashed line represents the position of 2 K, which is the limit of temperature of the susceptibility measurement.
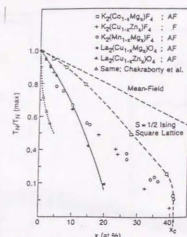
FIG. 3. Normalized Néel temperature (T_N/T_N(max)) vs concentration of nonmagnetic ions at magnetic sites in various quasi-2D magnets. (●, ▲: present work; Δ: from Ref. 8; the rest: from Ref. 1.) [T_N for ferromagnetic $K_2(Cu_{1-x}Zn_x)F_4$ stands for Curie temperature.]

Fig. 7-18

Néel temperature versus concentration of nonmagnetic impurities (Cheong et al. 1991).
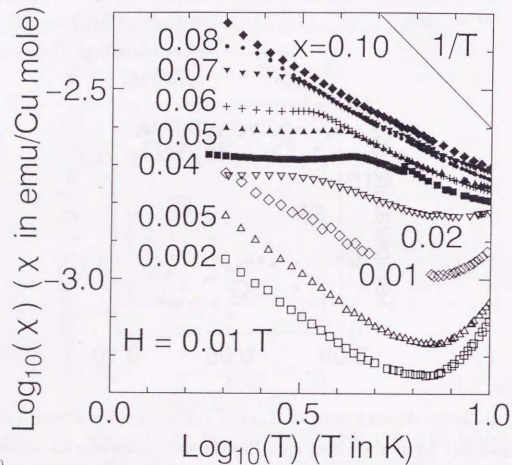
Fig. 7-19

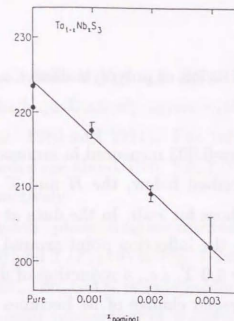$\log_{10}[\chi(T,x)]$ vs. $\log_{10}(T)$ below 10 K measured under $H=0.01$ T in the field-cooling process (Hase et al. 1993b).

54

Fig. 2 Concentration dependence of the transition temperature T_p in $Ta_{1-x} Nb_x S_3$ alloys. The full line leads to $dT_p/dc = 70$ K/at %

Fig. 7-20

Peierls transition temperature versus concentration of nonmagnetic impurities (Hsieh et al. 1983).

55

[7-4] High-field magnetization of polycrystalline $Cu_{1-x}Zn_xGeO_3$

The data of M for $x=0.005$ measured in increasing static H are shown in Fig. 7-21. As is described below, the H and T dependences of M for $x=0.005$ are similar to those for $x=0$. In the data at 2.5 K, we observed the rapid change of M with the inflection point around 12.0 T. We also saw a nonlinearity of M below 8.0 T, *i.e.*, a reduction of dM/dH with increasing H. As T is raised, the rapid change of M becomes suppressed and M *vs.* H is nearly linear up to 15 T above 12.9 K. The data of M *vs.* H becomes linear below 8.0 T with increasing T and shows a strong T dependence. This is consistent with the T dependence of the magnetic susceptibility $[\chi(T)]$ in 0.01 T (Hase *et al.* 1993b). On the other hand, M above 18.0 T is a linear function of H and is independent of T. Below 12.9 K, the slope of M in a high-field region is larger than that in a low-field region. As will be seen later, the hysteresis between M's in increasing and decreasing H's was observed below about 7.0 K. As is seen in Figs. 7-22 and 7-23, the data for $x=0.010$ and 0.020 exhibit similar properties.

The data of M measured at constant temperatures in increasing static H are shown in Figs. 7-24 $\sim$ 7-27. In the data at 4.2 K (Fig. 7-25), as x increases, the value of M increases and the change of M associated with the phase transition is suppressed. The x dependence of M in a high-field region is weaker than that in a low-field region. In particular the slope of M above 18.0 T is nearly independent of x.

The phase boundaries of $Cu_{1-x}Zn_xGeO_3$ are shown in Fig. 7-28. The data above and below 5.5 T represent H_c determined from M in this work and the H dependence of the SP transition temperature from $\chi(T)$ by the SQUID magnetometer, respectively. The value of H_c is nearly independent of T at low T in each sample and decreases upon doping. The

difference between the values of H_c^{up} and H_c^{down} ($H_c^{up} > H_c^{down}$) increases with decreasing T, which qualitatively agrees with the results of organic SP materials (Bloch *et al.* 1980 and 1981). The values of T below which the transition is of first order are about 10.0, 7.0, 7.0 and 2.4 K for $x=0$, 0.005, 0.010 and 0.020, respectively.

We show the magnetic phase diagram expressed in terms of the reduced variables $gH/2T_{SP}(0)$ and $T/T_{SP}(0)$ in Fig. 7-28(b). We assumed that the average g-value of $Cu_{1-x}Zn_xGeO_3$ is independent of x, because it mainly depends on the spin-orbit interaction of d electrons. The data of typical organic SP materials (Bloch *et al.* 1980 and 1981, and Northby *et al.* 1982a) and theoretical curves of Cross (1979) are also included in this figure. The magnetic phase diagrams of $Cu_{1-x}Zn_xGeO_3$ agree qualitatively with both experimental results of organic SP systems and the theoretical prediction except for a weak material dependence of the data at low T. As a result, we could determine the boundary between D and the other phases. It should be noted that the value of $gH_c/2T_{SP}(0)$ at low T slightly increases with doping, although the value of H_c itself at low T decreases.
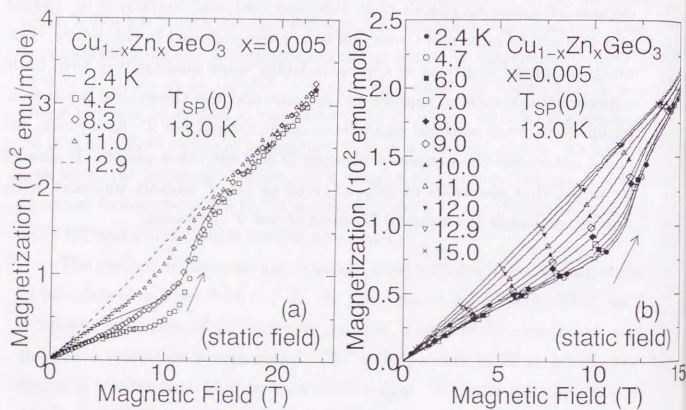
Fig. 7-21

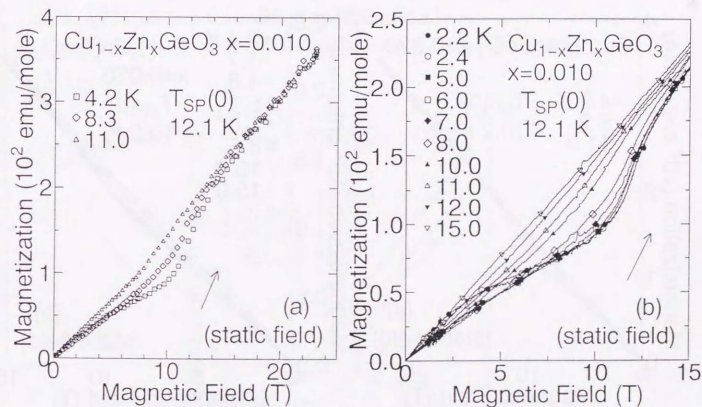The data of M with increasing static magnetic field of $Cu_{1-x}Zn_xGeO_3$: (a) $x=0.005$ up to 23 T (Hase *et al.* 1994) and (b) $x=0.005$ up to 15 T.

Fig. 7-22

The data of M with increasing static magnetic field of $Cu_{1-x}Zn_xGeO_3$: (a) $x=0.010$ up to 23 T and (b) $x=0.010$ up to 15 T.

Fig. 7-24

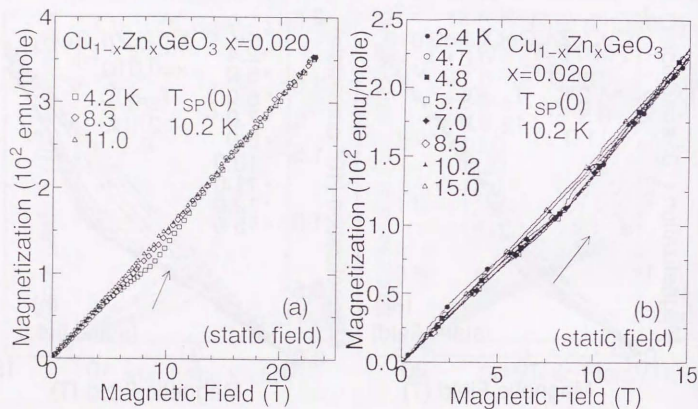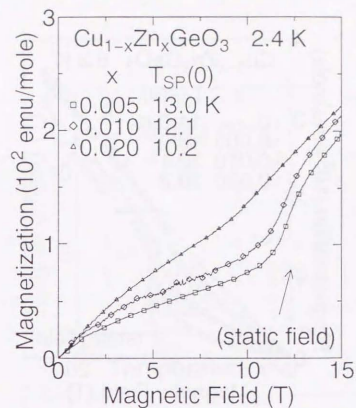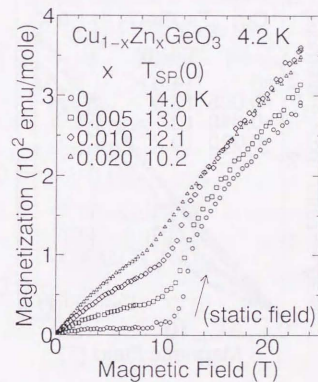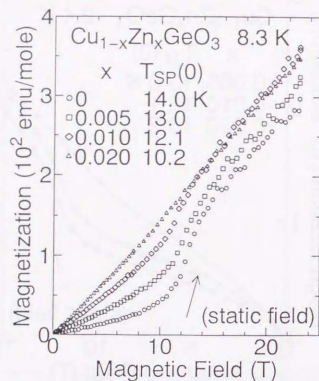The data of M with increasing static magnetic field at 2.4 K of $Cu_{1-x}Zn_xGeO_3$.

Fig. 7-25

The data of M with increasing static magnetic field at 4.2 K of $Cu_{1-x}Zn_xGeO_3$ (Hase *et al.* 1994).

Fig. 7-23

The data of M with increasing static magnetic field of $Cu_{1-x}Zn_xGeO_3$: (a) $x=0.020$ up to 23 T and (b) $x=0.020$ up to 15 T.
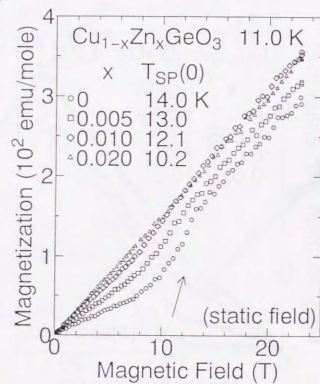
Fig. 7-26

The data of M with increasing static magnetic field at 8.3 K of $Cu_{1-x}Zn_xGeO_3$.

Fig. 7-27

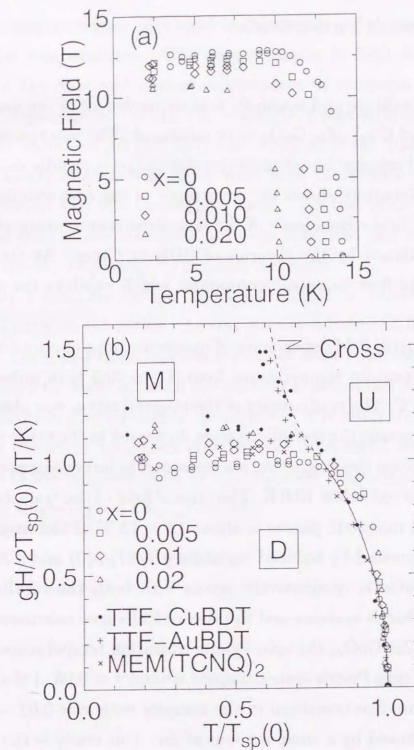The data of M with increasing static magnetic field at 11.0 K of $Cu_{1-x}Zn_xGeO_3$.

Fig. 7-28

The magnetic phase diagrams of $Cu_{1-x}Zn_xGeO_3$ (Hase *et al.* 1994): (a) H *vs.* T and (b) $gH/2T_{SP}(0)$ *vs.* $T/T_{SP}(0)$.

The temperature and magnetic field dependences of the magnetization of $CuGeO_3$ and $Cu_{1-x}Zn_xGeO_3$ were measured. The susceptibilities in the three principal orientations of single-crystal $CuGeO_3$ rapidly decrease below 14 K, which definitely shows the occurrence of the spin-Peierls transition. The magnetic field dependence of the transition temperature can be quantitatively explained by the theories of BBK or Cross. As far as I know, $CuGeO_3$ is the first inorganic compound which exhibits the existence of this transition.

The magnetic-field dependence of magnetizations of pure $CuGeO_3$ were measured at constant temperatures from 3.5 to 20.3 K in pulsed magnetic fields up to 25 T. The nonlinearity of the magnetization was observed below 13.4 K, which means the transitions from dimerized to the other phases. The hysteresis between the magnetization measured in increasing and decreasing fields was observed below 10.0 K. The critical field of the transition between dimerized and magnetic phases is about $12 \sim 13$ T. If the magnetic phase diagram is expressed by reduced variables $gH/2T_{SP}(0)$ and $T/T_{SP}(0)$, the diagram of $CuGeO_3$ qualitatively agrees with both the results of typical organic spin-Peierls systems and the theoretical curve calculated by Cross.

In $Cu_{1-x}Zn_xGeO_3$, the spin-Peierls transition temperature linearly reduces and the spin-Peierls state collapses around $x = 0.03$. I also discovered a new spin-glass-like transition in the samples with $x = 0.02 \sim 0.08$. This transition is caused by a small amount of Zn. This study is the first report of the effects of impurities on the spin-Peierls system.

In $Cu_{1-x}Zn_xGeO_3$, the characteristic change of the magnetization was observed below the spin-Peierls transition temperature, which means the phase transitions from dimerized to the other phases. The hysteresis be-

tween the magnetizations measured in increasing and decreasing fields was seen at low temperatures. The magnetization in high fields is a linear function of the field and almost independent of temperature, and shows a weak x dependence. When the magnetic phase diagram is expressed by reduced variables $gH/2T_{SP}(0)$ and $T/T_{SP}(0)$, the phase diagrams of $Cu_{1-x}Zn_xGeO_3$ qualitatively agree with both the results of organic spin-Peierls systems and the theoretical curve. As the value of x increases, the critical field of the transition between dimerized and magnetic phases (H_c^{DM}) reduces, while $gH_c^{DM}/2T_{SP}(0)$ increases.

Finally I describe further necessary studies to understand $CuGeO_3$ and its spin-Peierls transition. As was discussed before, a lattice distortion caused by the spin-Peierls transition has not been observed yet. Therefore it is necessary to study in detail the structural properties of this cuprate by X-ray or neutron measurements. In addition, it is interesting to investigate the newly discoverd spin-glass state by the differential susceptibility, the relaxation of the magnetization or the remanent magnetization, if possible, with using single-crystal $Cu_{1-x}Zn_xGeO_3$.

Acknowledgements

66

References

Adachi N. *et al.*, 1994, Proceedings of Todai Symposium 1993, 4th ISSP International Symposium, "FRONTIERS IN HIGH MAGNETIC FIELDS", to be published in Physica **B**.

Ajiro Y. *et al.*, 1989, Phys. Rev. Lett. **63**, 1424.

Binder K. and Young A. P., 1986, Rev. Mod. Phys. **58**, 801 (a review of the spin glass).

Bloch D. *et al.*, 1980, Phys. Rev. Lett. **44**, 294.

Bloch D. *et al.*, 1981, Phys. Lett. **82A**, 21.

Bonner J. C. and Fisher M. E., 1964, Phys. Rev. **135**, A640.

Bonner J. C. *et al.*, 1979, J. Appl. Phys. **50**, 1810.

Bonner J. C. and Blöte H. W. J., 1982, Phys. Rev. **B25**, 6959.

Bonner J. C. *et al.*, 1987, Phys. Rev. **B35**, 1791.

Bray J. W. *et al.*, 1975, Phys. Rev. Lett. **35**, 744.

Bray J. W., 1978, Solid State Commun. **26**, 771.

Bray J. W. *et al.*, 1979, Phys. Rev. **B20**, 2067.

Bulaevskii L. N., 1969, Sov. Phys. Solid State **11**, 921.

Bulaevskii L. N. *et al.*, 1972, Sov. Phys. JETP **35**, 384.

Bulaevskii L. N., Buzdin A. I. and Khomskii D. I., 1978, Solid State Commun. **27**, 5.

Cheikhrouhou A., Dupas C. and Renard J. P., 1983, J. Phys. Lett. **44**, L777.

Cheong S.-W., Thompson J. D. and Fisk Z., 1989, Physica **C158**, 109 (an example).

Cheong S.-W. *et al.*, 1991, Phys. Rev. **B44**, 9739.

Cross M. C. and Fisher D. S., 1979, Phys. Rev. **B19**, 402.

Cross M. C., 1979, Phys. Rev. **B20**, 4606.

67

de Jongh L. J. *et al.*, 1986, J. Magn. Magn. Mater. **54-57**, 1447.

des Cloizeaux J. and Pearson J. J., 1962, Phys. Rev. **128**, 2131.

Ginsberg D. M. (editor), 1992, Physical Properties of High Temperature Superconductors, (World Scientific, Singapore; a review).

Hagiwara M. *et al.*, 1990, Phys. Rev. Lett. **65**, 3181.

Haldane F. D. M., 1983a, Phys. Lett. **93A**, 464.

Haldane F. D. M., 1983b, Phys. Rev. Lett. **50**, 1153.

Hamamoto T. *et al.*, 1994, Proceedings of Todai Symposium 1993, 4th ISSP International Symposium, "FRONTIERS IN HIGH MAGNETIC FIELDS", to be published in Physica **B**.

Harada I. and Kotani A., 1982, J. Phys. Soc. Jpn. **51** 1737.

Hase M., Terasaki I. and Uchinokura K., 1993, Phys. Rev. Lett. **70**, 3651.

Hase M. *et al.*, 1993a, Phys. Rev. **B48**, 9616.

Hase M. *et al.*, 1993b, Phys. Rev. Lett. **71**, 4059.

Hase M. *et al.*, 1994, Proceedings of Todai Symposium 1993, 4th ISSP International Symposium, "FRONTIERS IN HIGH MAGNETIC FIELDS", to be published in Physica **B**.

Hijmans T. W., Brom H. B. and de Jongh L. J., 1985, Phys. Rev. Lett. **54**, 1714.

Hsieh P.-L. *et al.*, 1983, J. Phys. (Paris) Colloq. **44**, C3-1753.

Huizinga S. *et al.*, 1979, Phys. Rev. **B19**, 4723.

Inagaki S. and Fukuyama H., 1983a, J. Phys. Soc. Jpn. **52**, 2504.

Inagaki S. and Fukuyama H., 1983b, J. Phys. Soc. Jpn. **52**, 3620.

Inagaki S. and Fukuyama H., 1984, J. Phys. Soc. Jpn. **53**, 4386.

Interrante L. V. *et al.*, 1979, in Lecture Notes in Physics, **96** (Springer Verlag, Berlin) p. 55.

Izumi M. *et al.*, 1993, unpublished.

Jacobs I. S. *et al.*, 1976, Phys. Rev. **B14**, 3036.

Johnson J. D., Krinsky S. and McCoy B., 1973, Phys. Rev. **A8**, 2526.

Jordan P. and Wigner E. P., 1928, Z. Phys. **47**, 631.

Kasper J. S. and Moncton D. E., 1979, Phys. Rev. **B20**, 2341.

Katsumata K. *et al.*, 1989, Phys. Rev. Lett. **63**, 86.

Kikuchi J. *et al.*, 1994, submitted to J. Phys. Soc. Jpn.

Kuroe H. *et al.*, 1994a, to be published in J. Phys. Soc. Jpn.

Kuroe H. *et al.*, 1994b, unpublished.

Lu Z.-Y., Su Z.-B. and Yu L., 1993, preprint.

Luther A. and Peschel I., 1975, Phys. Rev. **B12**, 3908.

Luttinger J. M., 1963, J. Math. Phys. **4**, 1154.

Maeda A. *et al.*, 1990, Phys. Rev. **B41**, 4112 (an example).

Mekata M. *et al.*, 1987, J. Phys. Soc. Jpn. **56**, 4544.

Moncton D. E. *et al.*, 1977, Phys. Rev. Lett. **39**, 507.

Nakano T. and Fukuyama H., 1980, J. Phys. Soc. Jpn. **49**, 1679.

Nakano T. and Fukuyama H., 1981, J. Phys. Soc. Jpn. **50**, 2489.

Nishi M., Fujita O. and Akimitsu J., 1993, preprint.

Northby J. A. *et al.*, 1982a, Phys. Rev. **B25**, 3215.

Northby J. A. *et al.*, 1982b, J. Appl. Phys. **53**, 8032.

Petrakovskii G. A. *et al.*, 1990, Sov. Phys. JETP **71**, 772.

Pytte E., 1974, Phys. Rev. **B10**, 4637.

Ramirez A. P., Espinosa G. P. and Cooper A. S., 1990, Phys. Rev. Lett. **64**, 2070.

Renard J. P. *et al.*, 1987, Europhys. Lett. **3**, 945.

Roshen W. A., 1985, Phys. Rev. **B31**, 7296.

Schwerdtfeger C. F., Oostra S. and Sawatzky G. A., 1982, Phys. Rev. **B25**, 1786.

Shannon R. D. and Prewitt C. T., 1969, Acta Cryst. **B25**, 925.

Shannon R. D. and Prewitt C. T., 1970, Acta Cryst. **B26**, 1046.

Sugai S., 1993a, J. Phys. Soc. Jpn. **62**, 3829.

Sugai S., 1993b, preprint.

Tanaka Y., Satoh N. and Nagasaka K., 1990, J. Phys. Soc. Jpn. **59**, 319.

Terasaki I. *et al.*, 1994, unpublished.

Tomonaga S., 1950, Prog. Theor. Phys. **5**, 349.

van Bodegom B., Larson B. C. and Mook H. A., 1981, Phys. Rev. **B24**, 1520.

Völlenkle H., Wittmann A. and Nowotny H., 1967, Monatsh. Chem. **98**, 1352.

List of Papers of Our Group

M. Hase, I. Terasaki and K. Uchinokura,

"Observation of the spin-Peierls transition in linear Cu^{2+} (spin-$\frac{1}{2}$) chains in an inorganic compound $CuGeO_3$",

Phys. Rev. Lett. **70** (1993) 3651-3654.

M. Hase, I. Terasaki, K. Uchinokura, M. Tokunaga, N. Miura and H. Obara,

"Magnetic phase diagram of spin-Peierls cuprate $CuGeO_3$",

Phys. Rev. **B48** (1993) 9616-9619

(Technical Report of ISSP, Ser. A, No. 2696, June 1993).

M. Hase, I. Terasaki, Y. Sasago, K. Uchinokura and H. Obara,

"Effects of substitution of Zn for Cu in the spin-Peierls cuprate, $CuGeO_3$; The suppression of the spin-Peierls transition and the occurrence of a new spin-glass state",

Phys. Rev. Lett. **71** (1993) 4059-4062.

M. Hase, I. Terasaki, Y. Sasago, K. Uchinokura and H. Obara,

"Spin-Peierls transition in a cuprate, $CuGeO_3$",

Proceedings of the XXth International Conference on Low Temperature Physics, to be published in Physica **B**.

M. Hase, I. Terasaki, Y. Sasago, K. Uchinokura, M. Tokunaga, N. Miura and H. Obara,

"Effect of magnetic field on a spin-Peierls cuprate, $CuGeO_3$",

Proceedings of Molecular & Oxide Superconductors Conference. to be published in the Journal of Superconductivity.

M. Hase, I. Terasaki, Y. Sasago, K. Uchinokura, M. Tokunaga, N. Miura, G. Kido, T. Hamamoto and H. Obara,

"Magnetization of pure and Zn-doped spin-Peierls cuprate $CuGeO_3$ in high magnetic field",

Proceedings of Todai Symposium 1993, 4th ISSP International Symposium, "FRONTIERS IN HIGH MAGNETIC FIELDS", to be published in Physica **B**.

T. Hamamoto, G. Kido, M. Hase, Y. Sasago and K. Uchinokura,
"AC susceptibility in spin-Peierls compound $CuGeO_3$ under high magnetic fields",
Proceedings of Todai Symposium 1993, 4th ISSP International Symposium, "FRONTIERS IN HIGH MAGNETIC FIELDS", to be published in Physica **B**.

N. Adachi, T. Hamamoto, G. Kido, M. Hase, Y. Sasago, K. Uchinokura, S. Noro and T. Yamadaya,
"Far-infrared ESR study of cuprate compounds",
Proceedings of Todai Symposium 1993, 4th ISSP International Symposium, "FRONTIERS IN HIGH MAGNETIC FIELDS", to be published in Physica **B**.

T. Hamamoto, N. Adachi, G. Kido, M. Hase, Y. Sasago and K. Uchinokura,
"Phase diagram of spin-Peierls cuprate $CuGeO_3$ based on AC susceptibility in high magnetic fields",
to be published in J. Phys. Soc. Jpn.

H. Kuroe, K. Kobayashi, T. Sekine, M. Hase, I. Terasaki, K. Uchinokura,
"Heat capacity in an organic spin-Peierls system $CuGeO_3$",
to be published in J. Phys. Soc. Jpn.

J. Kikuchi, H. Yasuoka, H. Hase, Y. Sasago and K. Uchinokura,
"Cu nuclear quadrupole resonance study of $CuGeO_3$",
submitted to J. Phys. Soc. Jpn.